IMPACT OF MANGANESE ON CORROSION CONTROL AND BIOFILM FORMATION IN DISTRIBUTION SYSTEMS

by

Brittany Schae Gregory

Submitted in partial fulfilment of the requirements
for the degree of Master of Applied Science

at

Dalhousie University
Halifax, Nova Scotia
August 2017

TABLE OF CONTENTS

LIST OF TABLES vi

LIST OF FIGURES vii

ABSTRACT ix

LIST OF ABBREVIATIONS AND SYMBOLS USED x

ACKNOWLEDGEMENTS xii

Chapter 1: INTRODUCTION 1

1.1 PROJECT RATIONALE 1

1.2 RESEARCH OBJECTIVES 2

Chapter 2: LITERATURE REVIEW 3

2.1 OCCURRENCE OF MANGANESE IN NATURE 3

2.2 MANGANESE IN DRINKING WATER DISTRIBUTION 4

2.3 ACCUMULATION MECHANISMS 5

2.3.1 Physical and Chemical Accumulation of Manganese in Distribution 6

2.3.2 Biological Accumulation of Manganese in Distribution 7

2.4 CO-OCCURENCE OF MANGANESE WITH TRACE INORGANICS 9

2.4.1 Adsorption Mechanisms 9

2.4.2 Co-occurrence of Manganese with Lead 10

2.4.3 Application of Phosphate Based Corrosion Inhibitors 11

2.5 RESUSPENSION OF MANGANESE AND SUBSEQUENT ISSUES 12

2.5.1 Physical Release 12

2.5.2 Chemical Release 12

2.5.3 Biological Release 13

2.5.4 Taste and Odour 13

2.5.5 Neurotoxicity in School-aged Children 14

2.6 MANGANESE DRINKING WATER GUIDELINES 15
Chapter 3: MATERIALS AND METHODS 16
3.1 Source Water and Site Description 16
3.2 Annular Reactor Operation 16
3.3 Sample Collection and Water Quality Analysis 17
3.3.1 General Water Quality Analysis 18
3.3.2 Manganese and Lead Analysis 18
3.3.3 Phosphate Analysis 18
3.3.4 Natural Organic Matter Analysis 19
3.4 Biofilm Collection and Analysis 19
3.4.1 Adenosine Triphosphate Analysis 19
3.4.2 Manganese Oxidizing Bacteria Enumeration 20
3.4.3 Manganese Analysis 20
3.4.4 DNA Extraction and Sequencing 20
3.4.5 Scanning Electron Microscopy and Energy Dispersive Spectrometry 21
3.5 Statistical Analysis 21
Chapter 4: MANGANESE-BIOFOULING OF RAW WATER TRANSMISSION PIPELINES 22
4.1 INTRODUCTION 22
4.2 MATERIALS AND METHODS 23
4.2.1 Experimental Design & Set-Up 23
4.3 RESULTS AND DISCUSSION 26
4.3.1 Source Water Chemistry 26
4.3.2 Confirmation of Manganese-Biofouling in the Raw Water Transmission Pipe 27
4.3.3 Impact of System Changes on Biofilm Accumulation 31

4.3.3.1 Impact of Flow Rate Increase on Biofilm Accumulation 33

4.3.3.2 Impact of Cold Water Conditions on Biofilm Accumulation 34

4.3.3.3 Impact of Oxidation Enhancement on Biofilm Accumulation 35

4.4 CONCLUSIONS 37

Chapter 5: IMPACT OF PHOSPHATE AND MANGANESE ON BIOFILM ACCUMULATION ONTO POLYCARBONATE SURFACES 39

5.1 INTRODUCTION 39

5.2 MATERIALS AND METHODS 40

5.2.1 Experimental Design & Set-Up 40

5.3 RESULTS AND DISCUSSION 43

5.3.1 Source Water Chemistry 43

5.3.2 Impact of Manganese and Phosphate on Biofilm Accumulation 43

5.3.3 Proposed Role of Phosphate on Manganese and Biofilm Formation 49

5.3.3.1 Removal of Bulk Water Manganese 50

5.3.3.2 Comparison of Nitric Acid Preservation and Nitric Acid Digestion 52

5.4 Conclusions 54

Chapter 6: IMPACT OF RESIDUAL PHOSPHATE AND MANGANESE ON DOWSTREAM LEAD PIPES 56

6.1 INTRODUCTION 56

6.2 MATERIALS AND METHODS 57

6.2.1 Experimental Design & Set-Up 57

6.3 RESULTS AND DISCUSSION 59

6.3.1 Source Water Chemistry 59

6.3.2 Impact of residual manganese and phosphate on flowing water in lead pipes 59

6.3.3 Impact of residual manganese and phosphate on stagnated lead pipes 62

6.4 Conclusions 65
Chapter 7: CONCLUSION 67
7.1 Synthesis and Conclusions 67
7.2 Recommendations 68
REFERENCES 70

LIST OF TABLES

Table 3.1 Average raw and finished water quality at the JD Kline Water Supply Plant. . 16

Table 4.1 Average raw water quality conditions measured from May 2016 to April 2017 at the pumping station and pilot plant intakes. 26

Table 4.2 Average atomic composition (%) of the pumping station and pilot plant's polycarbonate coupon surface elements obtained through EDS analysis. 30

Table 4.3 Average atomic composition (%) of the control and pumping station reactors' polycarbonate coupon surface elements obtained through EDS analysis. . 36

Table 5.1 Summary of the experimental conditions and timeline for each annular reactor. 41

Table 5.2 Average influent water quality of the eight experimental conditions. 43

Table 5.3 Average atomic composition (%) of the polycarbonate coupon surface elements obtained through EDS analysis for the 0.7 and 1.2 mg-PO_4/L doses. 46

Table 5.4 Comparison of average manganese concentrations measured from nitric acid preservation and nitric acid digestion methods. 52

Table 6.1 Average lead pipe influent water quality for each experimental condition. 59

Table 6.2 Average turbidity and bulk water lead concentrations for each experimental condition sampled from the flowing water effluent and following the 6-hour stagnation. 64

Table 7.1 Key findings from each experimental approach. 67

LIST OF FIGURES

Figure 2.1 Manganese accumulation and release mechanisms in distribution. 5

Figure 4.1 Annular reactors operating in (A) the pumping station and (B) the pilot plant at the JD Kline Water Supply Plant. 24

Figure 4.2 Summary of the experimental conditions for each annular reactor. 25

Figure 4.3 Raw water manganese and DOC trends at the pumping station and pilot plant intakes from May 2016 to April 2017. 27

Figure 4.4 The percent reduction in bulk water manganese observed across the raw water transmission pipe throughout the experiment. 28

Figure 4.5 Biofilm accumulation on the polycarbonate coupons. 29

Figure 4.6 Biofilm analysis of total manganese, manganese oxidizing bacteria and tATP, measured on the surface of the polycarbonate coupons over the course of the experiment 30

Figure 4.7 Total manganese and manganese oxidizing bacteria densities, measured on the surface of the polycarbonate coupons during each experimental phase. 32

Figure 4.8 Manganese accumulation onto the polycarbonate surfaces over time, separated by experimental phase. 33

Figure 4.9 Biomass accumulation measured on the surface of the polycarbonate coupons for each experimental phase. 34

Figure 5.1 The experimental set-ups for both experimental phases. Phase 1 required the addition of phosphate, while phase 2 required the removal of phosphate through ferric (oxyhydr)oxide) filter columns. 42

Figure 5.2 Biofilm accumulation on the polycarbonate coupons following 8-weeks of treatment under all experimental conditions. 44

Figure 5.3 Total manganese and manganese oxidizing bacteria surface densities, measured on the polycarbonate coupons for each experimental condition. 45

Figure 5.4 Matched data points for manganese densities and plate counted manganese oxidizing bacteria measured on the polycarbonate coupon surfaces. 47

Figure 5.5 Biomass accumulation, measured on the surface of the polycarbonate coupons for each experimental condition. Error bars represent the 95% confidence interval. 49

Figure 5.6 Conceptual drawing of the effect of low phosphate (A) and high phosphate (B) doses on bulk water manganese and the formation of biofilm. 50

Figure 5.7 Estimated percent of manganese removed from the bulk water phase for each experimental condition. 51

Figure 5.8 Estimated mass of unaccounted for manganese for each experimental condition, calculated through system mass balances. 52

Figure 5.9 Unaccounted for manganese and adjusted manganese mass balances, comparing nitric acid preservation and nitric acid digestion methods. 53

Figure 6.1 The harvested lead-pipe sections (A), and the experimental set-up, with annular reactor discharge being fed into the lead-pipe sections (B). 58

Figure 6.2 The evolution of effluent manganese and lead over the experimental period measured under the 6-hour stagnation, high manganese, 1.2 mg-PO_4 condition. 60

Figure 6.3 Distribution of (A) bulk water manganese concentrations and (B) bulk water lead concentrations for each flowing water experimental condition. 61

Figure 6.4 Distribution of (A) bulk water manganese concentrations and (B) bulk water lead concentrations for each 6-hour stagnation experimental condition. 63

Figure 6.5 Turbidity samples measured from (A) the flowing pipe discharge and (B) the 6-hour stagnation period obtained under the low manganese, 0.7 mg-PO_4/L experimental condition. 64

ABSTRACT

Manganese in drinking water has typically been viewed as an aesthetic nuisance, owing to its tendency to cause water discoloration in its oxidized form. However, public health concerns regarding manganese is growing. Not only have manganese deposits been shown to scavenge a variety of trace inorganics, but emerging epidemiological studies have correlated manganese in drinking water with neurotoxicity in children. Accordingly, Health Canada has finalized new drinking water guidelines, lowering the aesthetic objective from 50 μg/L to 20 μg/L and creating a maximum acceptable concentration of 120 μg/L.

The fate of manganese in distribution, along with its potential impact on biomass accumulation and lead release was investigated in two distinct bench scale experiments. A study at the JD Kline Water Supply Plant in Halifax, Nova Scotia used untreated source water to confirm manganese-biofouling of their raw water transmission pipeline, demonstrating the importance of manganese oxidizing bacteria on the accumulation of manganese in distribution. A second experimental study investigated the impact of phosphate and manganese concentrations on manganese-biofilm accumulation in distribution. Lead pipe sections were run in series of this study, to determine the impact of residual manganese and phosphate on lead release.

Bench scale results found manganese accumulation increased from 32.67 μg/cm^2 to 115.93 μg/cm^2 across the JD Kline Water Supply Plant's raw water transmission pipeline. Manganese oxidizing bacteria were strongly correlated with these deposits ($\rho = 0.880$, $P<0.0001$), confirming manganese-biofouling of the pipeline. Increasing phosphate doses reduced manganese accumulation onto polycarbonate surfaces by 91.3%, decreasing from 32.8 μg/cm^2 to 2.9 μg/cm^2. Lead pipes exposed to manganese experienced greater lead release, with lead concentrations increasing from 573 μg/L at the low manganese level to 1048 μg/L at the high manganese level. Following stagnation, these lead concentrations increased to 7121 μg/L and 13 754 μg/L, respectively. Lead release was shown to decrease with increasing phosphate dose; however, the differences were not found to be significant. These results demonstrate the complex role of manganese in distribution systems, emphasizing the importance of manganese removal during treatment.

LIST OF ABBREVIATIONS AND SYMBOLS USED

δ-MnO_2	vernadite
µg	micrograms
AO	aesthetic objective
AR	annular reactor
ATP	adenosine triphosphate
CFU	colony forming units
cm	centimeter
Cl_2	chlorine
DI	deionized water
DNA	deoxyribonucleic acid
DO	dissolved oxygen
DOC	dissolved organic carbon
GCDWQ	Guidelines for Canadian Drinking Water Quality
EDS	energy dispersive spectrometry
HDPE	high-density polyethylene
ICP-MS	inductively coupled plasma mass spectrometry
IQ	intelligence quotient
IQR	interquartile range
JDKWSP	J.D. Kline Water Supply Plant
$KMnO_4$	potassium permanganate
MAC	maximum acceptable concentration
mg	miligrams
mL	millilitres
ML	million litres
Mn	manganese
$MnSO_4$	manganese (II) sulphate
MOB	manganese oxidizing bacteria
N	newton
NaOCl	sodium hypochlorite

NTU	nephelometric turbidity units
ORP	oxidation reduction potential
Pb	lead
PBS	phosphate buffered solution
pg	picogram
PO_4	phosphate
pH	potential of hydrogen (hydrogen potential)
PVC	polyvinyl chloride
RPM	revolutions per minute
TOC	total organic carbon

ACKNOWLEDGEMENTS

I would like to thank my supervisor, Dr. Gagnon for providing me the opportunity to complete this research, as well as his encouragement and guidance throughout the process. I am sincerely grateful to Nicole Allward for her endless support and her willingness to teach me everything I now know about microbiology. I would also like to thank everyone at the CWRS at Dalhousie University for their advice and support throughout my research, especially Tarra Chartrand, Allison Mackie and Yu Ri Park. Finally, I would also like to acknowledge the support of the staff at the JD Kline Water Supply Plant, who were very welcoming and willing to provide assistance during this project.

Chapter 1: INTRODUCTION

1.1 PROJECT RATIONALE

Following iron, Manganese (Mn) is the second most abundant transition metal on earth and is a common constituent in surface and groundwater systems due to weathering and leaching of Mn-bearing rocks (Groschen et al., 2009; Post, 1999). In the past, Mn regulatory limits for drinking water quality have been based on its ability to cause black water events at concentrations greater than the current Guidelines for Canadian Drinking Water Quality (GCDWQ) aesthetic objective (AO) of 50 μg/L (Health Canada, 2017). However, Mn has been shown to accumulate in distribution at influent concentrations as low as 20 μg/L (Kohl & Medlar, 2006) and can re-enter the bulk water phase with hydraulic or chemical changes in the system.

Public health concerns regarding Mn are rising, as it has been shown to be an efficient scavenger of trace inorganics including chromium, copper, strontium and lead (Dong et al., 2003; Manceau et al., 1992; McKenzie, 1980; Nelson et al., 1999; Villalobos et al., 2005) and an increasing number of studies have linked Mn in drinking water with neurotoxicity in school-aged children (Bhang et al., 2013; Bouchard et al., 2011; Henn et al., 2012; Khan et al., 2011; Kim, et al., 2009). Accordingly, Health Canada has finalized new Mn guidelines, lowering the AO to 20 μg/L to better manage Mn accumulation in distribution and creating a maximum acceptable concentration (MAC) of 120 μg/L to mitigate any potential health risks (Health Canada, 2016).

With a more stringent Mn guideline on the horizon and mounting public concern, a better understanding the fate of Mn in distribution and its interactions with inorganics, bacteria and added constituents like corrosion inhibitors is clearly necessary. While a variety of studies have investigated Mn accumulation in full scale distribution systems (Cerrato et al., 2006; Gerke et al., 2016; Schock et al., 2008, 2014; Sly et al., 1988, 1990), there has been limited research at the bench scale investigating the effects of various distribution conditions on Mn accumulation in a controlled setting.

1.2 RESEARCH OBJECTIVES

The fate of Mn in distribution was investigated at bench-scale using annular reactors (AR) and lead (Pb) pipe sections in two separate experimental designs. The first set-up used untreated source water at the JD Kline Water Supply Plant (JDKWSP) to confirm Mn-biofouling of their raw water transmission pipe. This set-up will demonstrate the importance of manganese oxidizing bacteria (MOB) in the accumulation of Mn in distribution, as well as the impact of water quality and hydraulic changes on biofilm densities. A second AR set-up used de-chlorinated tap water to study the impact of phosphate (PO_4) and Mn concentrations on Mn and biomass accumulation. Effluent from these reactors were fed directly into Pb-pipe sections to determine the effect of residual Mn and PO_4 on downstream Pb-pipes. In the past, Mn distribution research has predominantly focused on full-scale investigations. By preforming experiments in a controlled setting, the impact of a variety of system conditions could be investigated, which can then be broadly applied to other distribution systems.

The research objectives of this study are summarized below:

1. Evaluate manganese-biofouling of the JD Kline Water Supply Plant raw water transmission pipe and explore the impact of water quality and hydraulic changes on manganese and biomass accumulation;
2. Investigate the impact of various influent phosphate and manganese doses on manganese and biomass accumulation onto polycarbonate surfaces in distribution; and
3. Investigate the downstream impacts of residual phosphate and manganese on stagnant and flowing water in lead pipe.

Chapter 2: LITERATURE REVIEW

2.1 OCCURRENCE OF MANGANESE IN NATURE

Comprising 0.1% of the earth's crust, Mn is the second most abundant transition metal on earth and is prevalent in rock, soil and water (NAS, 1973). While it is not found in its elemental state in nature, Mn will form compounds over a wide range of oxidation states from -2 to +7, with Mn(II), Mn(IV) and Mn(VII) being the most commonly occurring species (Nealson et al., 1988). Mn occurs in both surface and groundwater through the weathering and leaching of Mn-bearing rocks and soils, and through anthropogenic activities such as ferroalloy production, smelting, fertilizing and landfill leaching (Kohl & Medlar, 2006; Stokes et al., 1988).

Thermodynamically, Mn(II) is the most stable state in fresh water and is a highly soluble and mobile species. However, the oxidation state of Mn is easily transformed depending on a variety of water quality properties such as pH, oxidation reduction potential (ORP), temperature, dissolved oxygen (DO) concentrations, and the presence of bacteria, organics, oxidants and other water constituents (Kohl & Medlar, 2006; Stokes et al., 1988). Under oxidizing conditions, soluble Mn(II) will convert to Mn(IV) which readily precipitates out of solution to form various manganese oxides and hydroxides (Brandhuber et al., 2015; Friedman et al., 2010; Kohl & Medlar, 2006; Sawyer et al., 2001). Changes in water quality can disrupt the stability of these precipitated Mn-oxides, resulting in the reduction of solid Mn(IV) to Mn(II), causing it to re-suspend in water (Hill et al., 2010).

Owing to a greater reduction potential within aquifers, dissolved Mn concentrations are typically higher in groundwater systems compared to surface waters. However, surface water Mn concentrations and speciation is far more variable and tends to fluctuate throughout bodies of water, especially during seasonal stratification. Following stratification, increased Mn(II) concentrations are observed below the thermocline, due to the low oxygen environment. Anoxic conditions promote the dissolution of Mn-oxides at the sediment-water interface, which can be facilitated by both chemical reactions and by

metal reducing bacteria (Nealson & Saffarini, 1994). Above the thermocline, oxygen at the air-water interface causes insoluble Mn(II) to oxidize to Mn(IV) and precipitate out of solution (Kohl & Medlar, 2006; MWH, 2005).

2.2 MANGANESE IN DRINKING WATER DISTRIBUTION

Due to its prevalence in groundwater and surface water, Mn is a common constituent in drinking water sources and must be removed through treatment prior to entering distribution. However, improper treatment techniques can also introduce Mn into the system through potassium permanganate ($KMnO_4$) oxidation, which is commonly used for Mn and iron removal (Kohl & Medlar, 2006). Mn concentrations well below the AO limit of 50 μg/L can be achieved through many treatment processes such as chemical oxidation followed by filtration, greensand adsorption or biofiltration (Tobiason et al., 2016). Residual Mn from water treatment facilities is available for release and accumulation in distribution systems (Kohl & Medlar, 2006; Sly et al., 1990).

The occurrence of Mn in distribution systems is well established in literature, demonstrating the widespread existence of Mn related issues. Sly et al. (1990) correlated Mn deposition with Mn bulk water concentrations and found that significant deposition occurred at Mn(II) concentrations as low as 30 μg/L. Kohl & Medlar (2006) compared Mn concentrations in distribution to those leaving treatment facilities and found that the average Mn concentration exiting treatment was 22 μg/L, regardless of treatment type, with a 90^{th} percentile concentration of 50 μg/L. In both studies, Mn bulk water concentrations decreased with distance from point of entry, implying the accumulation of Mn in distribution.

Manganese has been shown to accumulate on a variety of pipe material including lead (Gerke et al., 2016; Schock et al., 2008, 2014), iron (Cerrato et al., 2016; Peng et al., 2010) and polyvinyl chloride (PVC) (Cerrato et al., 2006; Peng et al., 2010; Sly et al., 1988, 1990), with its prevalence as a dominant scale component confirmed through the chemical analysis of scales detached from excavated distribution pipes. Peng et al. (2010)

found Mn to be the seventh most abundant element in iron and PVC pipe scales, with a median concentration of 790 µg/g, predominantly deposited as Mn-oxyhydroxides. An extreme case discovered by Friedman et al. (2010) found a high-density polyethylene (HDPE) pipe exposed to 0.05 mg-Mn/L over an 8-year period resulted in a thick, friable deposit comprised of 23.2% Mn by weight. Analyses of Pb-pipe sections found Mn-oxyhydroxide deposits ranging from 0.01 to 400 µm in thickness (Gerke et al., 2016) and Mn concentrations consistently over the reporting limit, reaching levels as high as 177 200 µg/g (Schock et al., 2008). An additional study by Schock et al. (2014) found Mn to account for 10% by weight of scale composition and that its presence hindered the formation of protective pattnerite minerals within the scales.

2.3 ACCUMULATION MECHANISMS

As depicted in Figure 2.1, the accumulation of Mn in distribution can be facilitated by a combination of physical, chemical and biological processes. The dominant mechanism is governed by system conditions, which in turn influences the rate and magnitude of Mn deposition. These governing conditions include, system hydraulics and water quality, the concentration and speciation of Mn in the bulk water, and the composition and properties of the solid substrate (Hill et al., 2010).

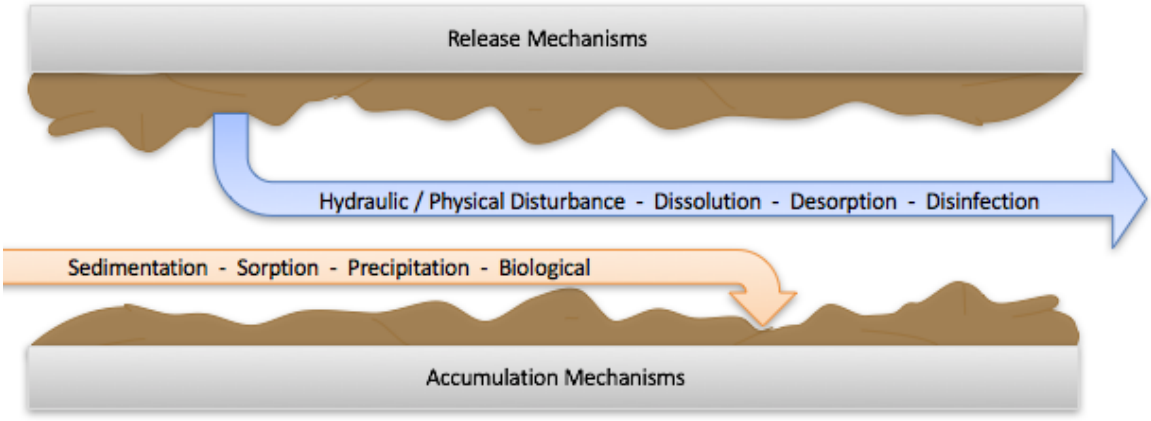

Figure 2.1 Manganese accumulation and release mechanisms in distribution.

2.3.1 Physical and Chemical Accumulation of Manganese in Distribution

Physical-chemical deposition and accumulation of Mn can occur through physical sedimentation by gravity, sorption and chemical precipitation (Hill et al., 2010). Mn(IV) deposits occur as a wide range of Mn oxides and hydroxides, all of which have open crystal structures. The open crystal structure allows for large surface areas that are extremely negative, resulting in high adsorption capacities. Mn(IV) solids readily partake in oxidation-reduction reactions and control the movement of Mn and its associated elements in distribution systems (Post, 1999; Tebo et al., 2004). These characteristics allow Mn oxides and hydroxides to be one of the strongest naturally occurring oxidizing compounds, aside from oxygen, in water (Tebo et al., 2004).

Particulate Mn(IV) can be physically deposited due to gravity under low-flow conditions, commonly found at dead-end and far-reaching sections within distribution systems (Brandhuber et al., 2015; USEPA, 2006). However, Mn bulk water concentrations are typically below the saturation limit for mineral phases (USEPA, 2006); therefore, physical sedimentation alone is unlikely to occur in distribution, unless accompanied by chemical oxidation as well.

Sorption encompasses both the adsorption of soluble Mn(II) onto solid phase substrates and absorption, the retention of Mn(II) within the structure of the substrates. Sorption is controlled by physical and electrostatic forces, as well as the chemical interactions between Mn(II) and solid surfaces like corrosion scales, sediment, precipitated Mn-oxides and biofilms (Brandhuber et al., 2015; Friedman et al., 2010; Schock, 2005). pH strongly influences surface charge and electrostatic interactions between Mn(II) and solid substrates, which in turn impacts the kinetic rate and extent of sorption. Bulk water Mn(II) concentrations and the presence of co-occurring contaminants will also affect the accumulation of Mn(II) by sorption. Co-occurring contaminants will compete with Mn(II) for surface space, which consequently reduces the substrate's capacity for Mn(II) ions (Friedman et al., 2010).

Chemical precipitation occurs when soluble Mn(II) becomes oxidized in distribution through increases in pH, ORP and DO, and in the presence of oxidizing agents such as ozone, chlorine disinfectants and $KMnO_4$ residuals. Once oxidized, Mn(II) converts to Mn(IV), which will precipitate out of the bulk water phase to form a variety of Mn oxides and hydroxides (Friedman et al., 2010; Knocke et al., 1990; Kohl & Medlar, 2006; Sly et al., 1990) and deposit onto interior pipe surfaces, corrosion scales and biofilms (Cerrato et al., 2006; Manceau et al., 1992; Schock et al., 2014). Co-precipitation is also a common accumulation mechanism, in which Mn(II) is adsorbed and enmeshed within the structure of an actively precipitating substrate (Friedman et al., 2010).

2.3.2 Biological Accumulation of Manganese in Distribution

Microorganisms such as bacteria, fungi and algae are known to oxidize Mn(II) in solution to Mn(III) and Mn(IV) (Ghiorse, 1984), and do so at a faster rate than oxidation facilitated by abiotic surface reactions (Hastings & Emerson, 1986; Nealson et al., 1988; Tebo, et al., 2004). The dominance of biologically mediated reactions over abiotic reactions in natural waters is likely due the high activation energy required for the oxidation of Mn(II) (Tebo et al, 2004). The bacteria known to catalyze the oxidation of Mn(II) in water are phylogenetically diverse; however, three model organisms are more frequently studied: the sheath forming *Leptothrix discophora* strain SS-1 (Ghiorse, 1987; Nelson et al., 1999), the spore forming *Bacillus* sp. (Cerrato et al., 2010; Dick et al., 2008; Hastings & Emerson, 1986; Mandernack et al., 1995) and *Pseudomonas putida* MnB1 and GB-1 (Villalobos et al., 2006; Caspi et al., 1998).

The oxidation of Mn(II) ions by MOB can occur through both direct and indirect oxidation processes. Bacteria may facilitate indirect Mn(II) oxidation by modifying pH and redox conditions in a localized area, or through the release of by-products that consequently cause chemical oxidation (Hullo et al., 2001; Tebo et al., 2004; Richardson et al., 1988). Direct oxidation processes occur through enzymatic intercellular oxidation, adsorption onto cell membrane surfaces and extracellular oxidation by excreted polysaccharides (Adams & Ghiorse, 1984; van Veen et al., 1978) or proteins (Ehrlich,

1968; Larson et al., 1999). Genetic sequencing of the three model organisms revealed that the genes used for Mn(II) oxidation share a sequence similar to those involved with multicopper oxidase enzymes (Dick et al., 2008; Francis et al., 2002).

While MOB have been shown to be resilient to a wide range of water conditions (Cerrato et al, 2010; Mandernack et al., 1995), their productivity is highly susceptible to water quality parameters such as pH, temperature, DO, and disinfectant concentrations. These parameters, along with a system's hydraulic conditions can affect the amount and diversity of MOB available to form active biofilms (Garny et al., 2008, Kohl & Dixon, 2012; Sly et al, 1988,1990). The impact of water velocity on MOB oxidation was demonstrated by Sly et al. (1988), who observed active Mn(II) oxidation at a velocity of 0.5 m/s; despite the bacteria being unable to do so at a velocity of 0.01 m/s. The low velocity microbial communities developed in mono-layers and had a greater diversity in comparison to the high velocity communities that formed in clumps and were encrusted in Mn-oxides.

Biogenic Mn-oxides produced by MOB vary by species, with *L discophora* producing sheaths, *Bacillus* sp. forming spores and *P. putida* producing biofilms (Tebo et al., 2004). The general structure of biogenic Mn-oxides has been shown to be layered phyllomanganates, with poor crystallinity and very high surface areas, most closely resembling vernadite (δ-MnO_2) or acid birnessite (Miyata et al., 2007; Post, 1999; Tebo et al., 2005). Due to their structure, these biogenic Mn-oxides have an extremely high sorption capacity for metal cations and can efficiently oxidize numerous inorganic and organic compounds (Miyata et al., 2007).

Despite the existence of MOB and the oxides they produce being well established in literature, the physiological function behind the oxidation process is still largely unknown. One theory speculates that MOB become encrusted in Mn-oxides that may serve as a form of protection from toxic metals, reactive oxygen, ultraviolet, predation and viruses (Ghiorse, 1984; Tebo et al., 2005). Biofilms encrusted in Mn have been shown to accumulate biomass at a faster rate than biofilms lacking Mn (Parikh et al.,

2005). Others have proposed that Mn oxidation has energy production benefits. Sunda & Kieber (1994) demonstrated that Mn-oxides degrade Humic substances to compounds that promote microbial growth and Tebo et al. (2005) suggested Mn(II) oxidation is energetically favourable, allowing that MOB to utilize the energy that is produced.

2.4 CO-OCCURENCE OF MANGANESE WITH TRACE INORGANICS

Manganese-oxides are known for their cation exchange capacity; accordingly, numerous studies have demonstrated Mn to be an effective scavenger of trace inorganics in water (Dong et al., 2003; Feng et al., 2007; McKenzie, 1980; Manceau et al., 1992; Nelson et al., 1999; O'Reilly & Hochella, 2003; Puppa et al., 2013; Wang et al., 2012; Zhao et al., 2010). Of the studies ranking the adsorption capacity of various trace metals onto metal oxides, a preferred association between Pb with Mn-oxides was observed over all other heavy metal and oxide substrate combinations (Feng et al., 2007; Manceau et al., 1992; McKenzie, 1980; O'Reilly & Hochella, 2003; Puppa et al., 2013; Wang et al., 2012).

2.4.1 Adsorption Mechanisms

Sorption of trace metals occurs within Mn-oxides to compensate for a negatively charged surface. These sorption mechanisms include adsorption onto the surface edges, the absorption into vacant sites or the substitution of Mn within the crystal lattice (O'Reilly & Hochella, 2003; Villalobos, 2005; Wang et al., 2012). Sorption is typically enhanced with increasing pH and when competitive cation concentrations are minimal. Zhao et al. (2010) found adsorption of Pb(II) onto δ-MnO_2 was dependant on pH, with adsorption increasing between pH 2-7, plateauing between 7-10 and sharply decreasing at pH greater than 10. Chen et al. (2000) found a similar Pb(II) adsorption dependence with pH, in addition to other factors such as ORP, exposure time, temperature, and the presence of competing cations and MOB as well.

2.4.2 Co-occurrence of Manganese with Lead

Wang et al. (2012) quantified the adsorption of Pb onto Mn-oxides to be 1.6 to 3.9 times greater than any of other the metals investigated. McKenzie (1980) found that the adsorption of Pb by synthetic Mn-oxides was up to 40 times greater than by iron-oxides. He also found no evidence of Pb oxidation or the formation of Pb-Mn minerals during adsorption. Similar studies found that Pb adsorption capacity of Mn-oxides exceeded that of iron-oxides by nearly an order of magnitude (Dong et al., 2003) and Pb binding capacity was greater on Mn-oxides compared to iron-oxides, regardless of their surface areas (Nelson et al., 1999; O'Reilly & Hochella, 2003).

Compared to those chemically produced, biogenic Mn-oxides adsorb a considerably greater amount of Pb. Sorption of Pb to Mn-oxides produced by *L. discophora* SS-1 was determined to be two to five times greater than to those chemically precipitated by $KMnO_4$ or commercially purchased (Nelson et al., 1999, 2002). Surface area was determined to be the contributing factor of Pb sorption, as the biogenic Mn-oxide produced by *L. discophora* had the largest specific surface area of 224 m^2/g due to its low crystallinity. By contrast, the chemically produced Mn-oxides surface area was 58 m^2/g and the commercial Mn-oxides ranged from 0.048-4.7 m^2/g (Nelson et al., 2002).

In Pb-service lines, Mn scale deposits have been shown to adsorb and mobilize Pb particles into distribution, resulting in increased Pb and Mn concentrations at consumer taps (Schock et al., 2014). Trueman & Gagnon (2016) were able to prove a similar mechanism between iron colloids and lead particles using high molecular weight elution profiles. These profiles demonstrated an apparent linear dependence ($R^2 = 0.82$) between the two, indicating iron rich colloids were mobilizing Pb. Since Pb has been shown to have a much higher affinity for Mn over iron, the same mechanism may be occurring between Pb and Mn.

2.4.3 Application of Phosphate Based Corrosion Inhibitors

Phosphates are effective corrosion inhibitors in drinking water distribution (Cartier et al., 2012; Kogo et al., 2017; Lytle & Schock, 1996; McNeill & Edwards, 2004; Volk at al., 2010; Woszczynski et al., 2015), with 56% of American water utilities reporting its application for corrosion control in 2001 (McNeill & Edwards, 2002). While typically applied for Pb control, phosphate can also be used to sequester Mn by preventing oxidation. Heintze (1968) confirmed the formation of manganese-orthophosphate compounds (Equation 1) that allow Mn to remain in solution and inhibits colloids from forming larger particles (Knocke et al., 1987; Kohl & Medlar, 2006; Sommerfield, 1999).

$$3Mn^{2+} + 2H_2PO_4^- + 4OH^- \rightleftharpoons Mn_3(PO_4)_2 4H_2O \qquad \text{(Equation 1)}$$

The application of polyphosphates in combination with chlorine is the most commonly reported method employed to sequester Mn (Friedman et al., 2010; Kohl & Medlar, 2006; Lytle & Schock, 2002; Sommerfield, 1999). Mn-oxides can obscure the role of phosphates in distribution, as they have been shown to exert a competitive demand on the phosphate ions, limiting its effectiveness as a corrosion inhibitor (Dalvi et al., 2015; Lytle & Snoeyink, 2002; Zhang et al., 2007). While the efficacy of phosphate as a corrosion inhibitor may be reduced in the presence of Mn-oxides, it has been shown to reduce the adsorption of heavy metals onto these oxides (Dalvi et al., 2015; Zhang et al., 2007).

Phosphate based corrosion inhibitors may have unintended consequences as a nutrient source for bacteria, enhancing bacterial cell growth in distribution (Chu et al., 2005; Jang et al., 2012; Lehtola et al., 2002; Payne, 2013; McNeill & Edwards, 2002). Increasing phosphorus has also been found to cause thicker, less homogenous biofilms with increased diversity, regardless of pipe material (Fang et al., 2009; Jang et al., 2012; Payne, 2013). While Fang et al. (2009) determined that bacterial cell counts increased 1-log with the addition of 30 μg/L of phosphorus, they also noticed a decrease in extracellular polymeric substance production. This leads to biofilms with larger surface

areas available for nutrient uptake; however, the weaker structure also makes them more susceptible to disinfection.

2.5 RESUSPENSION OF MANGANESE AND SUBSEQUENT ISSUES

Most accumulation mechanisms are fully reversible through physical disruptions, chemical dissolution, desorption, and biofilm inactivation (Figure 2.1). This can lead to contaminant release into drinking water, causing concentrations that may exceed the current drinking water quality guidelines and be of public health concern at customer taps. These release events have been observed and documented in several studies (Clement & Carlson, 2004; Reiber & Dostal, 2000; Reiber & Giani, 2005; Schock et al., 2008).

2.5.1 Physical Release

Sediments, chemical precipitates and biofilms can be dislodged by hydraulic and physical disturbances that entrain the solids in the bulk water phase (Friedman et al.; Hill et al., 2010). Physical release is often reported as the primary release mechanism in distribution (Clement & Carlson, 2004; Lytle et al., 2010; Schock, 2005) and can be caused by abrupt velocity increases, flow reversals, pressure transients, main breaks, earthwork and construction work (Friedman et al., 2003). Physical release is often identified through aesthetic quality deterioration, such as increased turbidity and discoloration. However, smaller scale releases, could result in elevated contaminant concentrations at the tap, with no visible aesthetic issues (Schock, 2005).

2.5.2 Chemical Release

The dissolution of precipitates occurs when changes in water chemistry disrupt the conditions in which the solids were formed, causing mineral instability. Treatment adjustments to pH, and disinfectant and phosphate concentrations can cause mineral transformation, scale instability and Mn-dissolution until equilibrium is re-established.

Large sections of distribution may be effected by dissolution over an extended period, with little to no aesthetic issues (Hill et al., 2010).

Manganese-oxide release through desorption occurs through competitive displacement and surface substitution by compounds of similar physical and electrochemical forms (USEPA, 2006). Switching water sources, blending water, treatment modifications and seasonal effects can cause the desorption and release of Mn (Hill et al., 2010). Mn has been shown to be associated with orthophosphate as well as organic and mobile fractions that can cause desorption through competitive displacement reactions (Friedman et al., 2010; Peng & Korshin, 2011). Co-precipitated or buried sediments may be more resilient to desorption into the bulk water phase (Shock, 2005).

2.5.3 Biological Release

Established biofilms are vulnerable to inactivation caused by temperature fluctuations and disinfection. Ginige et al. (2011) found biofilm activity on glass surfaces increased during the late summer and early fall, which corresponded with an increase in Mn deposition. Testing during the cooler months however, showed biofilm activity decreased by an order of magnitude, which subsequently lowered Mn biofilm concentrations as well. The same study showed that Mn incorporated in biofilms was susceptible to release upon inactivation through disinfection. Biofilm reactors dosed with Mn were exposed to chlorination which resulted in a ten-fold decrease in adenosine triphosphate (ATP) biofilm concentrations within a ten-day period.

2.5.4 Taste and Odour

Customer perception of safe drinking water is associated with taste, smell and appearance, with Mn being attributed to black-brown water, fixture and clothing staining, and a bitter metallic taste (Kohl & Medlar, 2006). Sain et al. (2014) studied the visual and taste thresholds for both Mn(II) and Mn(IV) at concentrations ranging from 0.005 to 506 mg/L and found that water dosed with 0.05 mg/L Mn(II) and Mn(IV) could not be distinguished by taste from distilled water. It was also found that the taste population

threshold for Mn(II) is 75-100 mg/L and that Mn(II) in solution remained visually undetectable at concentrations up to 506 mg/L. Mn(IV) on the other hand, is visually detectable at a concentration of 0.005 mg/L, clearly demonstrating the importance of Mn speciation on visual and taste thresholds.

2.5.5 Neurotoxicity in School-aged Children

Toxic exposure to Mn can cause manganism with symptoms similar to Parkinson's disease, and is typically associated with occupational settings (Brandhuber et al., 2015). However, a growing number of epidemiological studies have linked Mn consumption in drinking water with neurotoxicity in school-aged children (Bhang et al., 2013; Bouchard et al., 2011; Henn et al., 2012; Khan et al., 2011; Kim et al., 2009; Shin et al., 2015). Therefore, Mn release in distribution is not only problematic aesthetically, but also due to possible health concerns related to Mn consumption and its associated trace metals.

Bouchard et al. (2011) examined the relationship between Mn exposure from drinking water with children's intelligence quotient (IQ) scores. Comparisons of Mn exposure routes showed that Mn intake from water consumption is far more bioavailable than through food consumption, with IQ results showing that a ten-fold increase in Mn water concentrations, was associated with a 2.4 IQ point decrease. Other studies focusing on behavioural issues related to Mn consumption from drinking water found increased Mn concentrations were significantly associated with attention-deficit hyperactivity disorder (Shin et al., 2015) and withdrawn, anxious and aggressive behaviours (Khan et al., 2011).

Due to its affinity to scavenge trace inorganics, several studies have examined the impact of the co-exposure of Mn and Pb drinking water on neurotoxicity. When comparing blood Mn and Pb levels, with the IQ scores of school-aged children, an additive effect modification was found in one study (Kim et al., 2009) and a synergistic on neurodevelopmental problems were found in another (Henn et al., 2012). These results indicate that Pb toxicity could potentially increase among children already exposed to high Mn concentrations.

2.6 MANGANESE DRINKING WATER GUIDELINES

Due to its ability to cause black water events, and issues related to taste and odour, the current guideline for Mn in the GCDWQ is an AO of 50 μg/L. However, this guideline was last updated in 1987, and advances in water treatment and mounting public health concerns regarding Mn has led Health Canada to revaluate this contaminant limit. Health Canada has recently finalized new guidelines, lowering its AO to 20 μg/L and creating a MAC of 120 μg/L. By lowering the AO, Health Canada is hoping to reduce the number of dirty water complaints caused by Mn and improve consumer confidence in drinking water quality. The MAC will help mitigate potential health risks associated with drinking water consumption as research continues to develop on the topic (Federal-Provincial-Territorial Committee on Drinking Water, 2016).

Chapter 3: MATERIALS AND METHODS

3.1 Source Water and Site Description

Both the untreated and finished water used throughout this study was obtained from the J.D. Kline Water Supply Plant in Halifax, Nova Scotia. The JDKWSP uses Pockwock Lake, located within a protected watershed, as its source water supply. As shown in Table 3.1, Pockwock Lake is characterized by having a low pH, low alkalinity, and low turbidity (Halifax Water, 2016). The plant services 201 000 customers and has a design capacity of 220 ML/day, though the average daily intake is approximately 90 ML/day (Halifax Water, 2010). The JDKWSP operates as a direct filtration plant, using coagulation with alum followed by dual media filtration consisting of sand and anthracite as its main forms of treatment. Filtered water is then dosed with chlorine for disinfection, sodium hydroxide for pH adjustment and zinc orthophosphate for corrosion control. The average finished water quality parameters, prior to distribution, are also listed below in Table 3.1.

Table 3.1 Average raw and finished water quality at the JD Kline Water Supply Plant.

Parameter	Raw Water	Treated Water
Alkalinity (as $CaCO_3$)	<1.0 mg/L	22.5 mg/L
Hardness (as $CaCO_3$)	4 mg/L	11.2 mg/L
pH	5.8	7.3
Turbidity	0.3 NTU	< 0.09 NTU
Colour	16 NTU	< 3.0 NTU
TOC	2.6 mg/L	1.5 mg/L
Iron	< 0.06 mg/L	< 0.05 mg/L
Manganese	0.034 mg/L	0.008 mg/L
Lead	< 0.6 µg/L	< 0.5 µg/L

3.2 Annular Reactor Operation

Annular reactors are often used for biofilm accumulation studies to simulate drinking water distribution systems at the bench scale (Camper et al., 2003; Fang et al., 2009;

Gagnon et al., 2005; Garny et al., 2008; Jang et al., 2012; Payne, 2013; Rand et al., 2007; Rygel, 2006). The annular reactors (Biosurfaces Technologies Inc., Bozeman, MT) are completely mixed reactors consisting of an inner rotating polycarbonate drum surrounded by an outer glass cylinder. Shear stresses comparable to those found in distribution are controlled by a variable speed motor that rotates the inner drum, while the hydraulic retention times are controlled by the volumetric flow rate of the influent water. To support biofilm growth, 20 coupons are flush mounted on the inner rotating drum, which can later be removed for analysis.

Prior to their use, the annular reactors and coupons were cleaned and sterilized. First, the annular reactors and coupons were scrubbed with phosphorus free soap and rinsed with deionized water (DI). The coupons were then soaked in a 10% nitric acid solution to remove any remaining metals and rinsed with DI. The sterilization procedure for the annular reactors was adapted from multiple studies (Fang et al., 2009; Payne, 2013; Rygel, 2006). The reactors were assembled, with the coupons in place, and autoclaved at 121°C for 15 minutes. The tubing was then set up, and the reactors were flushed with 70% ethanol for 24 hours and rinsed with DI. Following sterilization, flow breaks were added to prevent back flow contamination and all the non-opaque surfaces were covered with aluminum foil to reduce phototrophic growth within the reactors (Gagnon et al., 2005; Rand et al., 2007; Rygel et al., 2006).

3.3 Sample Collection and Water Quality Analysis

All aqueous samples were collected in 500 mL HDPE bottles, which were soaked in a 10% nitric acid solution for 24 hours and rinsed 3 times with DI water prior to their use. Samples collected from the JDKWSP were stored in an ice-packed cooler for transport to Dalhousie University for further analysis.

3.3.1 General Water Quality Analysis

Temperature and pH were measured immediately following sampling using an Accumet XL-60 double junction electrode (Fisher Scientific, MA, USA). A three-point calibration at pH 4, 7 and 10 was performed each day prior to its use. Turbidity was measured using a turbidimeter (2100N Turbidimeter, HACH, CO, USA), according to the manufacturer's instructions.

3.3.2 Manganese and Lead Analysis

Manganese and lead were analyzed using inductively coupled plasma mass spectrometry (ICP-MS) (X-Series 2 ICP-MS, Thermo Fisher Scientific, MA, USA), which has a minimum detection level of 0.4 μg/L for lead and 0.8 μg/L for manganese. Water samples were transferred to 14 mL polyethylene vials and acidified with trace metal nitric acid to a pH < 2 for preservation. Samples collected form the Pb-pipe sections often had a turbidity greater than 1-NTU; therefore, were prepared for analysis using nitric acid digestion in accordance to Standard Methods 3030E (APHA, 2012). A portion of the samples were processed by AGAT Laboratories (Dartmouth, Nova Scotia) using ICP-MS in accordance to Standard Method 3125. The laboratory's reporting detection level for manganese and lead were 2 μg/L and 0.5 μg/L, respectively.

3.3.3 Phosphate Analysis

Phosphate was measured using ion chromatography (761 Compact IC, Metrohm, Herisau, Switzerland), which has a method detection limit of 0.7 mg/L. Samples below this detection limit were occasionally analyzed with a HACH DR5000 (HACH, CO, USA) using the PhosVer 3 method (#8048), which can detect orthophosphate at concentrations between 0.02 and 2.50 mg/L.

3.3.4 Natural Organic Matter Analysis

Natural organic matter was measured as total organic carbon (TOC), dissolved organic carbon (DOC) and as colour. TOC samples were collected in 40-mL glass vials with zero headspace and preserved with phosphoric acid to pH < 2. DOC samples were filtered through preconditioned 0.45-µm cellulose filter membranes prior to collection and preservation. Samples were then analyzed using a Shimadzu TOC-VCSH TOC Analyzer (Shimadzu, Kyoto, Japan) using the combustion catalytic oxidation/NDIR TOC-V method. The minimum detection limit of organic carbon is 0.25 mg/L. True colour was measured with a HACH DR5000 (HACH, CO, USA) using the Platinum-Cobalt Standard Method (#8025).

3.4 Biofilm Collection and Analysis

Annular reactor coupons were acclimated for a 30-day period prior to sample collection, to ensure stable biofilm growth (Gagnon et al., 2015; Rand et al., 2007; Payne, 2013). The coupons were aseptically removed with a flame sterilized metal hook and immediately placed in autoclaved 150 mL test tubes. Coupons removed from the JDKWSP were placed in autoclaved 150 mL test tubes filled with effluent water to prevent the biofilm from drying out. The tubes were then stored in an ice-packed cooler for transport to Dalhousie University for further analysis. All microbiological analyses were performed in a biosafety cabinet to limit sample contamination. Following analysis, the coupons were rinsed with DI and sterilized with 70% ethanol. Once dried, they were returned to the annular reactor.

3.4.1 Adenosine Triphosphate Analysis

Adenosine Triphosphate analysis was performed on one third of the coupon surface, measuring approximately 7.5 cm^2, using LuminUltra Technologies' (New Brunswick, Canada) Deposit & Surface Analysis Test Kit. The analyses were conducted in accordance to the manufacturer's surface swab protocol. Relative light units were

measured using a Kikkoman C-100 LumiTester (Tokyo, Japan) and were converted to pg/cm^2 using the manufacturer's provided formula.

3.4.2 Manganese Oxidizing Bacteria Enumeration

Manganese oxidizing bacteria were quantified using one third of the coupon surface, measuring approximately 7.5 cm^2. As described by Payne (2013) biofilm was gently scraped into sterilized test tubes using an autoclaved spatula, and rinsed with 1 mL of sterilized phosphate buffered solution (PBS). The suspended biofilm was then vortexed to homogenize the solution. Ten-fold dilutions to 10^{-4} were spread plated, in triplicate, using 0.1 mL of sample in accordance with Standard Methods 9215C (APHA, 2012). The culture media was composed of R2A agar spiked with 17 mg/L $MnSO_4$ (Fisher Scientific, ON) to encourage MOB growth as described by Burger et al. (2008). The plates were then incubated in the dark for a 30-day period at room temperature, after which time black MOB colonies could be identified and enumerated.

3.4.3 Manganese Analysis

The remaining third of the biofilm was gently scraped from the coupons into 50-mL test tubes and rinsed with 50 mL of DI. The samples were prepared for analysis using nitric acid digestion in accordance to Standard Methods 3030E (APHA, 2012), with the manganese analysis being performed with an X-Series 2 ICP-MS (Thermo Fisher Scientific, MA, USA).

3.4.4 DNA Extraction and Sequencing

Upon experimental completion, coupons were aseptically removed from the reactors for biofilm DNA extractions. The coupons were gently scrapped with an autoclaved spatula into sterilized test tubes and rinsed with 10 mL of sterilized DI. The samples were then centrifuged at 10 000 x g for 30 seconds and the supernatant was decanted. The cells were rinsed an additional three times following the same procedure. After the final rinse, the supernatant was decanted and the DNA was extracted from the pellet using the

MoBio PowerBiofilm DNA Isolation kit (MoBio Laboratories, Inc., California, USA) in accordance with the manufacturer's protocol. Following DNA extraction and quantification, the samples were sent to the Centre of Comparative Genomics and Evolutionary Bioionformatics at Dalhousie University for 16s rRNA sequencing and species identification.

3.4.5 Scanning Electron Microscopy and Energy Dispersive Spectrometry

An additional coupon was removed from the reactors at the end of the experimental period and placed in a desiccator for future scanning electron microscopy and energy dispersive spectrometry (EDS) analysis. Preparations for analysis included cutting and plating the coupons and coating them with 27 nanometers of gold. The scanning electron microscope (Hitachi S-4700 FE-SEM, Hitachi Ltd, Tokyo, Japan) includes an energy dispersive X-ray analysis system, which was used to analyze the atomic and weight percent composition of three locations on each of the coupon surfaces.

3.5 Statistical Analysis

Microsoft Excel® (Microsoft, Redmond, WA, U.S.A.) was used for data organization, analysis and the calculation of confidence intervals. All other statistical analyses were performed using Minitab Express ® software (MINITAB Inc., State College, PA, USA), which included mean comparisons using paired t-tests and Tukey's method, as well as Pearson correlation testing. All statistical analyses were conducted at the 95% confidence level.

Chapter 4: MANGANESE-BIOFOULING OF RAW WATER TRANSMISSION PIPELINES

4.1 INTRODUCTION

Water quality samples taken from the JD Kline Water Supply Plant's pumping station and treatment plant intakes revealed that bulk water Mn concentrations were decreasing between the two locations. Manganese accumulation, caused by biofouling of the supply plant's raw water transmission pipe, was blamed for the observed reduction. The 48-inch pipe, which is 1051 m in length and constructed of lined concrete, is used to transport raw water from the pumping station to the supply plant for treatment prior to distribution. Halifax Water, the operators of the supply plant, expressed interest in confirming Mn-biofouling of the transmission pipe and exploring the impact of water quality and hydraulic changes on Mn and biomass accumulation.

The accumulation of Mn in distribution has been well established in literature, demonstrating the widespread occurrence of Mn related issues in drinking water systems. Studies investigating the fate of Mn in distribution found the concentration of bulk water Mn decreased with distance from its point of entry, implying deposition within the system (Kohl & Medlar, 2006; Sly et al., 1990). This accumulation has been confirmed by studies examining the chemical composition of excavated pipe scales, with results showing Mn to be a dominant component in scales obtained from pipes composed of Pb (Gerke et al., 2016; Schock et al., 2008, 2014), iron (Cerrato et al., 2016; Peng et al., 2010) and PVC (Cerrato et al., 2006; Peng et al., 2010; Sly et al., 1988, 1990). In terms of abundance, Schock et al. (2014) found Mn to account for 10% by weight of scale removed from lead pipes, while Friedman et al. (2010) found Mn to account for 23.2% by weight of scale from an HDPE pipe exposed to 50 μg/L over an 8-year period.

Depending on the water quality and hydraulic conditions within a system, Mn accumulation can be facilitated by a combination of physical, chemical and biological processes. Other important factors impacting the rate of deposition include the concentration and speciation of bulk water Mn and the composition of the solid substrate

(Hill et al., 2010). These factors are particularly important in surface waters, as Mn concentrations and speciation tend to fluctuate throughout bodies of water, especially during seasonal stratification (Kohl & Medlar, 2006; MWH, 2005). Since the source water is not disinfected prior to entering the transmission pipe at the JDKWSP, biogenic oxidation is likely the principle accumulation mechanism in this system. Oxidation facilitated by bacteria has been shown to dominate abiotic reactions in natural waters (Hastings & Emerson, 1986; Nealson et al., 1988; Tebo et al., 2004), likely due to the high activation energy required for the oxidation of Mn(II) (Tebo et al, 2004).

The issue with Mn accumulation in distribution arises from its tendency to re-enter the bulk water phase through physical disruptions, chemical dissolution, desorption, and biofilm inactivation (Clement & Carlson, 2004; Reiber & Dostal, 2000; Reiber & Giani, 2005; Schock et al., 2008). While this would be problematic on its own, the affinity for Mn-oxides to scavenge trace inorganics in water exacerbates the issue even further (Dong et al., 2003; Feng et al., 2007; McKenzie, 1980; Manceau et al., 1992; Nelson et al., 1999; O'Reilly & Hochella, 2003; Puppa et al., 2013; Wang et al., 2012; Zhao et al., 2010). At the JDKWSP, the release of accumulated Mn within the raw water transmission pipe could cause unexpected spikes in Mn requiring treatment, along with its associated bacteria and trace inorganics.

4.2 MATERIALS AND METHODS

4.2.1 Experimental Design & Set-Up

To confirm Mn-biofouling of the raw water transmission pipe, an annular reactor was set up at the JDKWSP pumping station intake to simulate the transmission pipe's hydraulic conditions. A second reactor was set up following the transmission pipe at the JDKWSP pilot plant, to compare Mn and biofilm densities between the two locations. These reactors operated under the same hydraulic conditions throughout the experiment, simulating the transmission pipe's low demand flow rate of 65 million liters per day. Within the reactors, this flow rate was equivalent to a 27.2-minute hydraulic retention time, operating at a speed of 217 RPM, as determined by the manufacturer's operations

manual. Influent water in the pumping station was drawn from the raw water intake, whereas the pilot plant reactor was fed water from the pilot plant's influent over flow (Figure 4.1).

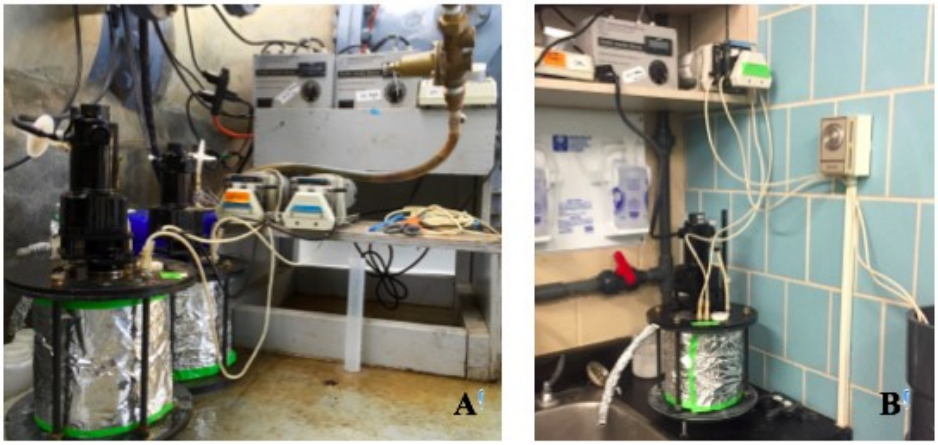

Figure 4.1 Annular reactors operating in (A) the pumping station and (B) the pilot plant at the JD Kline Water Supply Plant.

In addition to the confirmation of Mn-biofouling of the raw water transmission pipe, the impact of four experimental conditions on Mn and biomass accumulation were investigated during this study (Figure 4.2). This required the employment of a third annular reactor, operating in parallel to the pumping station reactor to compare the effects of system changes on biofilm growth. During the first phase of the experiment, the reactor was operated under JDKWSP's low demand flow rate condition of 65 million liters per day for a period of ten weeks. The impact of flow rate increases was then investigated by operating the reactor under JDSKWSP's high demand flow rate of 100 million liters per day over a 17-week period. This flow rate was simulated with a 17.7-minute hydraulic retention time, at an operating speed of 407 RPM, as determined by the manufacturer's operations manual. As water temperatures dropped below 14°C, the impact of cold water temperatures on Mn and biomass accumulation could be studied. During this 15-week phase, the reactor was operated under the low demand flow rate. The final condition studied was the impact of oxidant enhancement on Mn accumulation taking place over a 7-week period. Sodium hypochlorite (NaOCl) was dosed at 0.15 mg-Cl_2/L, as determined through breakpoint testing of the source water. The sodium

hypochlorite stock solutions were prepared using autoclaved DI water and was replaced weekly.

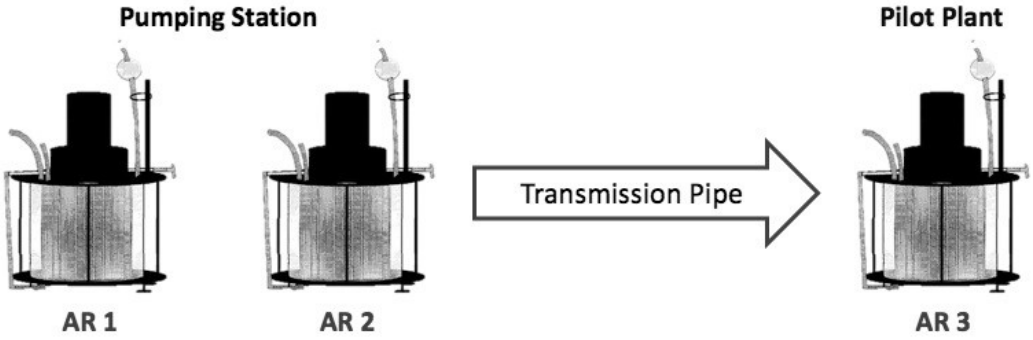

	Phase 1 10 weeks	**Phase 2** 17 weeks	**Phase 3** 15 weeks (Winter)	**Phase 4** 7 weeks
AR 1	Low Demand (65 million L/day)			
AR 2	Low Demand (65 million L/day)	High Demand (100 million L/day)	Low Demand (65 million L/day)	Low Demand Oxidant Enhancement
AR 3	Low Demand (65 million L/day)			

Figure 4.2 Summary of the experimental conditions for each annular reactor.

Polycarbonate coupons were used during this study as a substitute to lined-concrete, as it is an inert material and often used in biofilm reactor studies (Sharp, 2001; Garny, et al., 2008; Graham et al., 2005, Camper, 2005; Fang et al., 2009, Rand et al., 2007). Results obtained using polycarbonate coupons serve as a conservative estimate to the results that would have been obtained with lined concrete coupons, as studies have shown polycarbonate accumulates the least amount of biomass compared to other pipe materials (Camper et al., 2003; Gagnon et al., 2005).

The coupons were removed bi-weekly for sampling, with the exception of December-March. During this time, coupon sampling occurred monthly, as Mn concentrations (Granger, 2013) and biomass activity (Ginige, 2011; Kohl & Medlar, 2006; Lauderdale et al., 2016) have been shown to decrease under cold water conditions. Coupons were transported to Dalhousie University in sterile test tubes filled with effluent water and later

analyzed for Mn, MOB and tATP, as described in Chapter 3: Following experimental completion, scanning electron microscopy, EDS and DNA extraction for future sequencing were also performed on the coupons. Influent and effluent bulk water samples were collected weekly for pH, temperature, turbidity and total manganese analysis, while additional analyses of TOC, DOC and colour were performed on a bi-weekly basis. During the cold-water phase, bulk water sampling was reduced to a bi-weekly basis. Temperature, pH and turbidity were analyzed immediately following sampling at the JDKWSP lab, while the remaining analyses were performed at Dalhousie University. All materials and methods used during this study are detailed in Chapter 3:

4.3 RESULTS AND DISCUSSION

4.3.1 Source Water Chemistry

Raw water from the pumping station and pilot plant intakes were sampled and characterized over a 49-week period from May 2016 to April 2017, with the results summarized in Table 4.1.

Table 4.1 Average raw water quality conditions measured from May 2016 to April 2017 at the pumping station and pilot plant intakes.

Parameter	Pumping Station	Pilot Plant
Manganese (µg/L)	34.02 ± 14.62	29.63 ± 25.08
Temperature (°C)	14.9 ± 4.1	15.8 ± 3.4
pH	5.25 ± 0.43	5.10 ± 0.53
Turbidity (NTU)	0.790 ± 0.51	0.733 ± 0.50
DOC (mg/L)	3.260 ± 0.33	2.99 ± 0.361
TOC (mg/L)	3.530 ± 0.49	3.08 ± 0.741
Colour (NTU)	14 ± 10	15 ± 14

At both intakes, Mn concentrations were typically below the AO limit of 50 µg/L, excluding a few unexpected spikes at the pilot plant as shown in Figure 4.3. These spikes are likely the result of biofilm resuspension in the transmission pipe, as there were no corresponding Mn increases observed at the pumping station intake during these events. Temperatures at the pumping station varied from 7.0°C in January to 21.4°C in August,

averaging 14.9°C, while the pilot plant intake was slightly warmer, averaging 15.8°C. Mn concentrations varied somewhat over the course of the experiment, with a 10 µg/L increase observed at the beginning of November. DOC results followed a very similar trend, reaching a minimum concentration at the beginning of November. By sampling over the winter months, the impact of cold water temperatures on MOB efficiency and Mn accumulation could be evaluated.

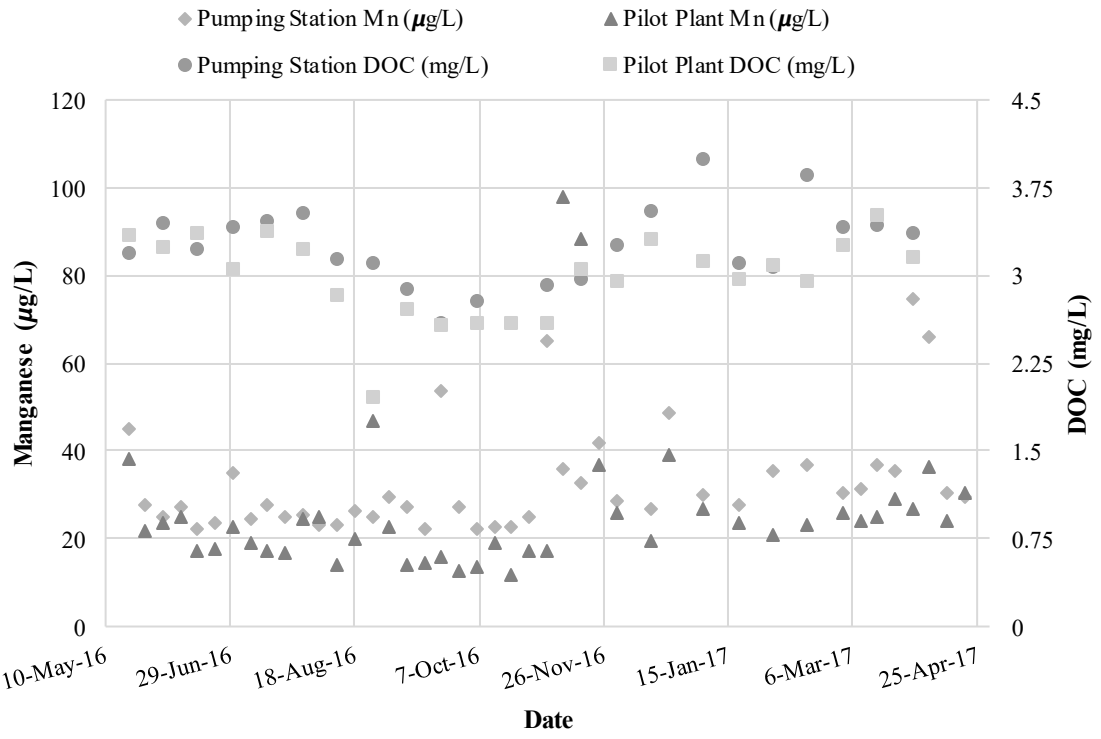

Figure 4.3 Raw water manganese and DOC trends at the pumping station and pilot plant intakes from May 2016 to April 2017.

4.3.2 Confirmation of Manganese-Biofouling in the Raw Water Transmission Pipe

Upon discovering an apparent decrease in bulk water Mn concentrations across the raw water transmission pipe at the JDKWSP, Halifax Water began testing Mn at the pumping station and treatment plant intakes on a semi-regular basis using the HACH 1-(2-Pyridylazo)-2-Naphthol PAN Method (#8149). The results of Halifax Water's data

collection, as well as the data collected throughout the study were used to confirm the reduction in bulk water Mn across the pipe, as shown in Figure 4.4.

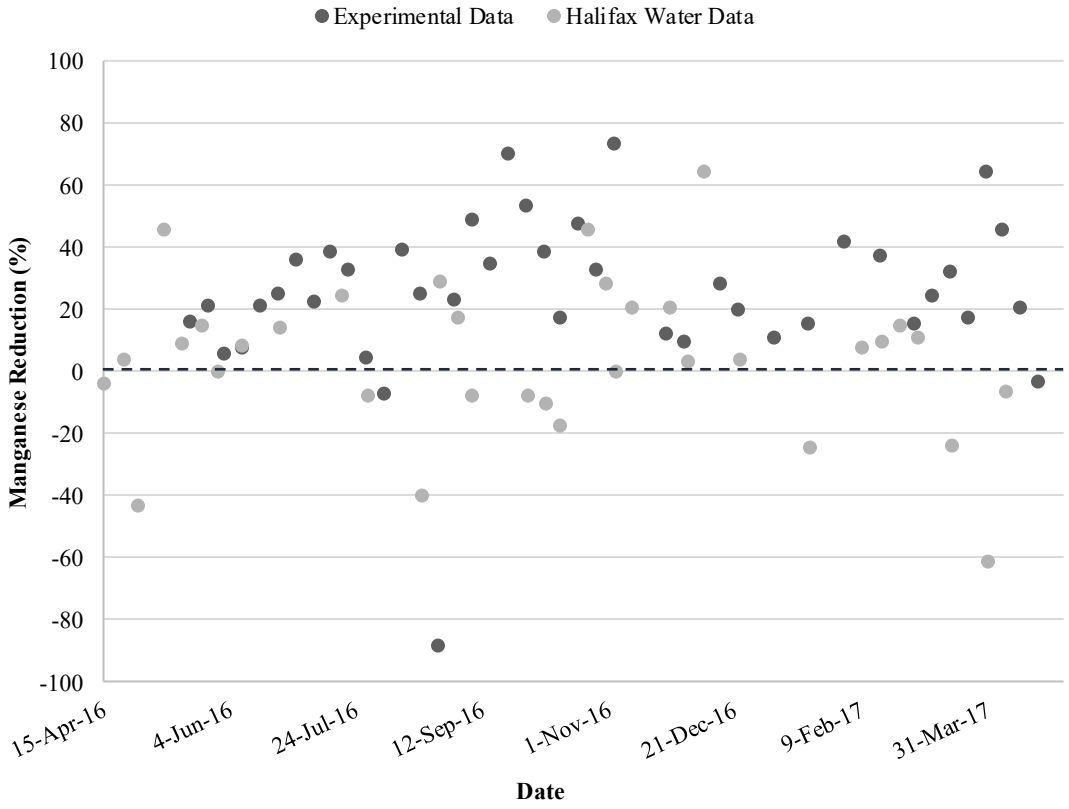

Figure 4.4 The percent reduction in bulk water manganese observed across the raw water transmission pipe throughout the experiment.

The majority of the sampling events saw a reduction in Mn across the transmission pipe (62.9% from the Halifax Water data and 88.3% from the experimental data), with an observed average reduction of 6.3 µg/L. However, only the experimental data was found to have a significant difference in Mn across the transmission pipe (P=0.0333), perhaps due to the larger data set or the use of different analytical methods. The reduction in bulk water Mn between the two intakes suggests Mn is accumulating within the transmission pipe, which is supported by previous distribution studies that found bulk water Mn concentrations decreased with distance from the point of entry due to Mn accumulation (Sly et al., 1990; Kohl & Medlar, 2006).

Polycarbonate coupons have been shown to accumulate the least amount of biomass when compared to other pipe materials (Camper et al., 2003; Gagnon et al., 2005); therefore, were used as a conservative proxy for the transmission pipe material in this study. A visible inspection of the coupons, as seen in Figure 4.5, indicate Mn accumulation occurred within each system. Black dots, identified as Mn deposits, can be observed on all three coupon surfaces, with the pilot plant coupons amassing the greatest amount of biofilm over the course of the experiment.

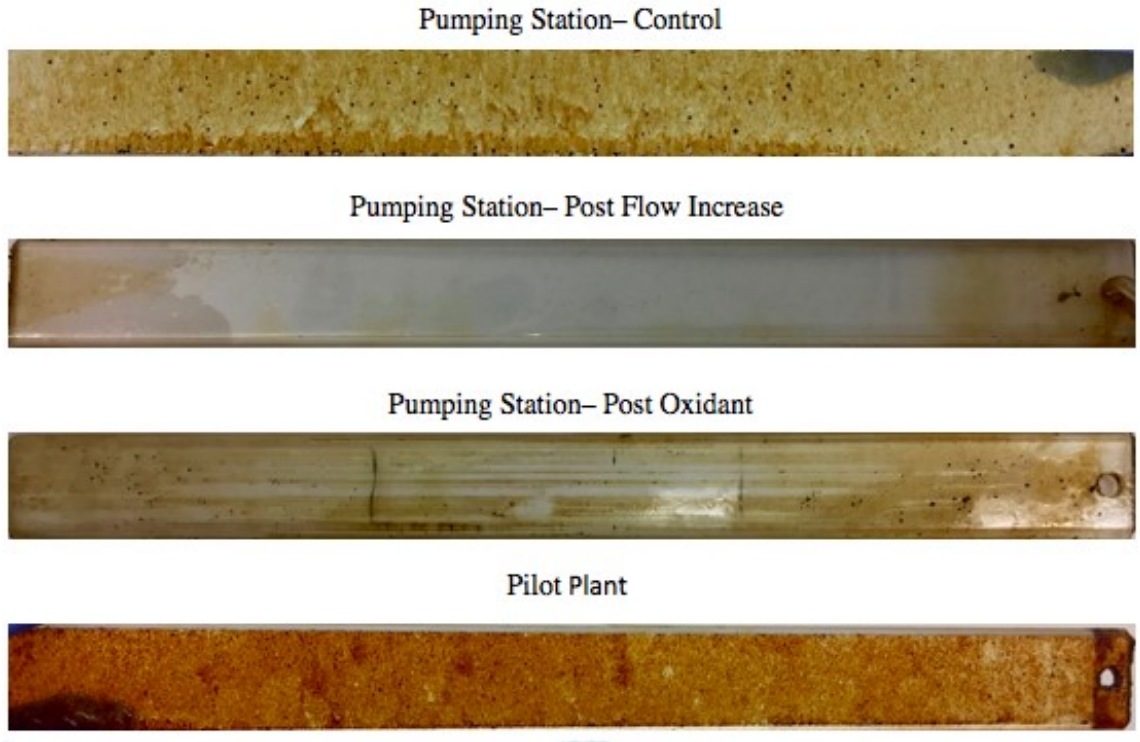

Figure 4.5 Biofilm accumulation on the polycarbonate coupons.

Confirmation of Mn accumulation onto polycarbonate surfaces was achieved through chemical analysis of the accumulated biofilms. Figure 4.6 shows the Mn surface density results within the pumping station and pilot plant reactors over the course of the experiment. An average Mn surface density of 10.96 $\mu g/cm^2$ was observed within the pumping station, reaching a final density of 32.67 $\mu g/cm^2$. In comparison, the average pilot plant surface density was significantly higher ($P=0.0003$) at 36.16 $\mu g/cm^2$, reaching a final density 115.93 $\mu g/cm^2$. An EDS analysis of the coupon surfaces also confirmed

the presence of Mn within the biofilm (Table 4.2). Results show an average percent atomic composition of 1.03% in the pumping station reactor, which more than doubled to 2.53% within the pilot plant reactor.

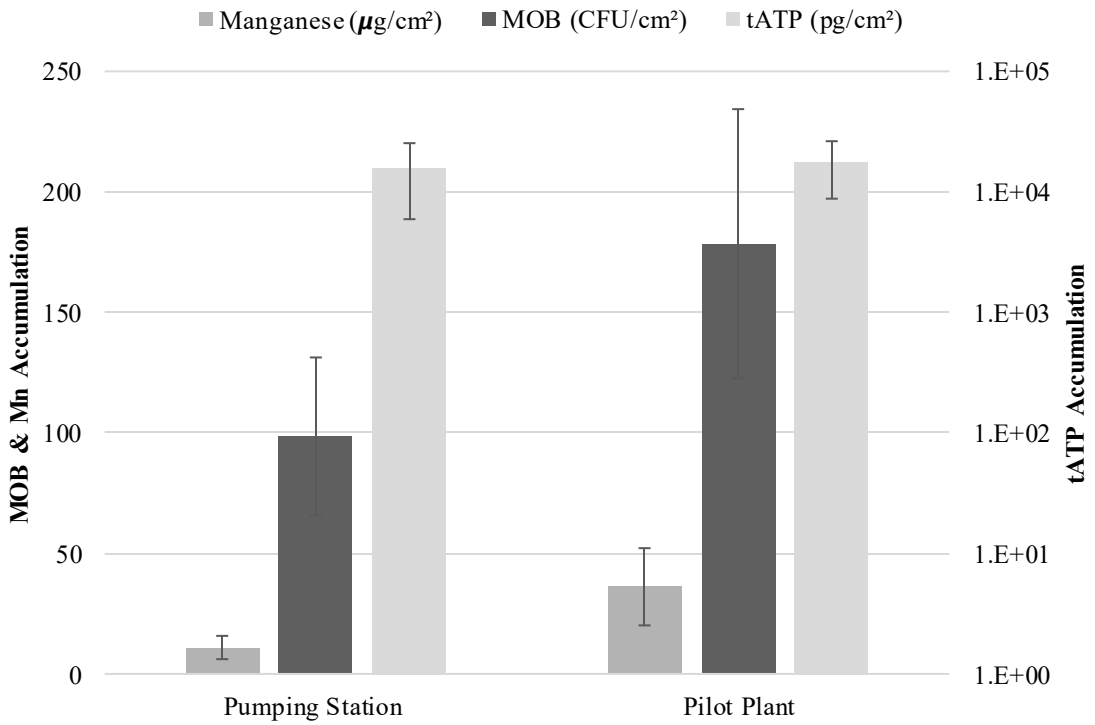

Figure 4.6 Biofilm analysis of total manganese, manganese oxidizing bacteria and tATP, measured on the surface of the polycarbonate coupons over the course of the experiment. Error bars represent the 95% confidence interval.

Table 4.2 Average atomic composition (%) of the pumping station and pilot plant's polycarbonate coupon surface elements obtained through EDS analysis.

	% Atomic Composition							
	C	**N**	**O**	**Al**	**Si**	**Cl**	**Mn**	**Fe**
Pumping Station	62.91	4.37	29.54	0.33	0.58	0.05	1.03	1.18
Pilot Plant	53.31	6.10	36.03	0.64	0.19	0.00	2.53	1.19

Culturable MOB within the biofilm were enumerated through spread plating to confirm biologically facilitated Mn oxidation. The spread plate results, seen in Figure 4.6, show that the average MOB surface density increased significantly following the raw water transmission pipe ($P < 0.0001$), increasing by nearly 80% to 178 CFU/cm^2. A Pearson correlation coefficient showed a significant ($\rho = 0.880$, $P<0.0001$) relationship between Mn and MOB surface densities on the coupon surfaces. This strong correlation suggests MOB are facilitating the oxidation of Mn onto the polycarbonate surfaces, especially given the unfavourable oxidation conditions caused by the acidic pH. Ginige et al. (2011) found a significantly positive correlation between biological activity and Mn deposition in distribution. Granger (2013) also found a similar positive correlation between heterotrophic plate counts and increased Mn removal in biofilters, concluding that removal was likely due to biological oxidation.

Biological oxidation would explain how the pilot plant reactor accumulated more than triple the amount of Mn compared to the reactor located in the pumping station, despite having significantly lower influent Mn concentrations. The MOB present within the pilot plant reactor likely originated from the transmission pipe, where established active biofilms can easily be removed by hydraulic disturbances. For example, Halifax Water performs quarterly line flushes, which could dislodge biofilm within the transmission pipe biofilm and transport it to the pilot plant reactor where it can quickly re-establish active MOB colonies. This would allow for MOB and Mn to accumulate at a faster rate compared to the pumping station reactor, which would have to establish MOB colonies from planktonic bacteria.

4.3.3 Impact of System Changes on Biofilm Accumulation

The impact of water quality and hydraulic changes on biofilm accumulation was observed through an increase in flow rate, operation under cold water conditions and oxidant enhancement. The average cumulative Mn and MOB results obtained from each experimental phases are displayed in Figure 4.7, while Figure 4.8 shows Mn

accumulation over time in both reactors to compare deposition rates under each experimental condition.

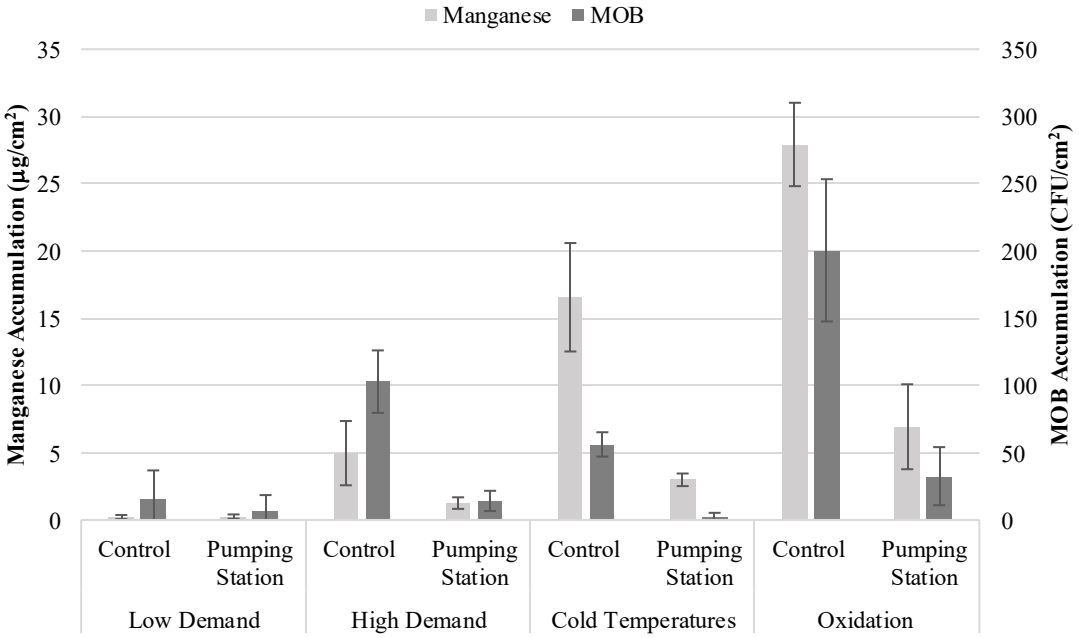

Figure 4.7 Total manganese and manganese oxidizing bacteria densities, measured on the surface of the polycarbonate coupons during each experimental phase. Error bars represent the 95% confidence interval.

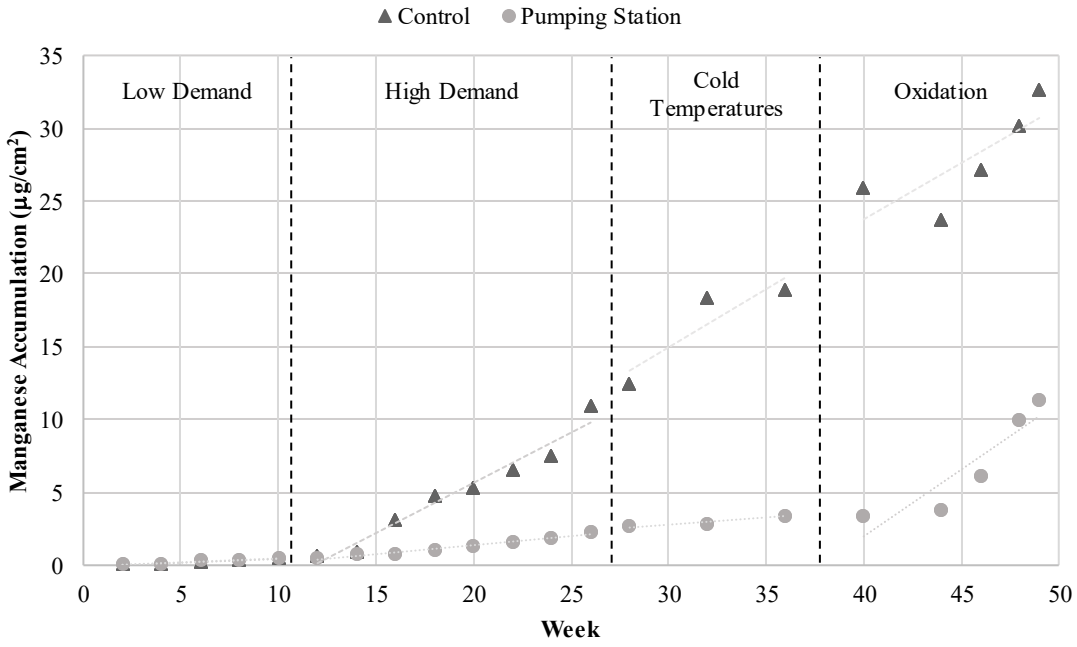

Figure 4.8 Manganese accumulation onto the polycarbonate surfaces over time, separated by experimental phase.

4.3.3.1 Impact of Flow Rate Increase on Biofilm Accumulation

During the low demand flow rate, the biofilm analyzed from the pumping station and control reactors were statistically similar (Figure 4.7). However, following the flow rate increase to high demand, Mn and MOB surface densities were significantly lower than those measured from the control coupons. When compared to the low demand results, the increased flow rate coupons accumulated a quarter of the Mn and 7.4 times less MOB. The increased flow rate also resulted in Mn accumulating at a much slower rate compared to the control. As seen in Figure 4.8, Mn accumulated at a rate of approximately 0.69 µg/cm^2 per week within the control reactor, while only accumulating 0.12 µg/cm^2 per week at the higher flow rate.

As hydraulic disturbances are commonly cited as a primary removal mechanism in distribution (Clement & Carlson, 2004; Lytle et al., 2010; Schock, 2005), the decrease in biofilm was likely the result of physical removal caused by the increase in shear stress. Friedman et al. (2003) came to a similar conclusion, finding that diurnal demand patterns

can mobilize loose biofilm on pipe surfaces. The lower rate of accumulation following the flow rate increase was likely due to the high shear stress and low hydraulic retention time in the system, creating less favourable conditions for biofilm growth.

4.3.3.2 Impact of Cold Water Conditions on Biofilm Accumulation

The optimum temperature for MOB growth is approximately 30°C (Ghirose, 1984; Mandernack et al., 1995; Kielemoes, et al., 2002), although the optimum range has been described to be as wide as 15-30°C (Tipping, 1984). Unsurprisingly, as water temperatures dropped to as low as 7.0°C during the winter phase, bacterial growth was negatively impacted. MOB concentrations were decimated within the pumping station reactor, while concentrations decreased significantly from 103 CFU/cm^2 to 56 CFU/cm^2 in the control. A similar decrease in bacterial growth from 170 CFU/cm^2 to 121 CFU/cm^2 was observed in the pilot plant reactor during this time. tATP results, which indicate microbial population, also showed no significant bacterial growth during this phase (Figure 4.9).

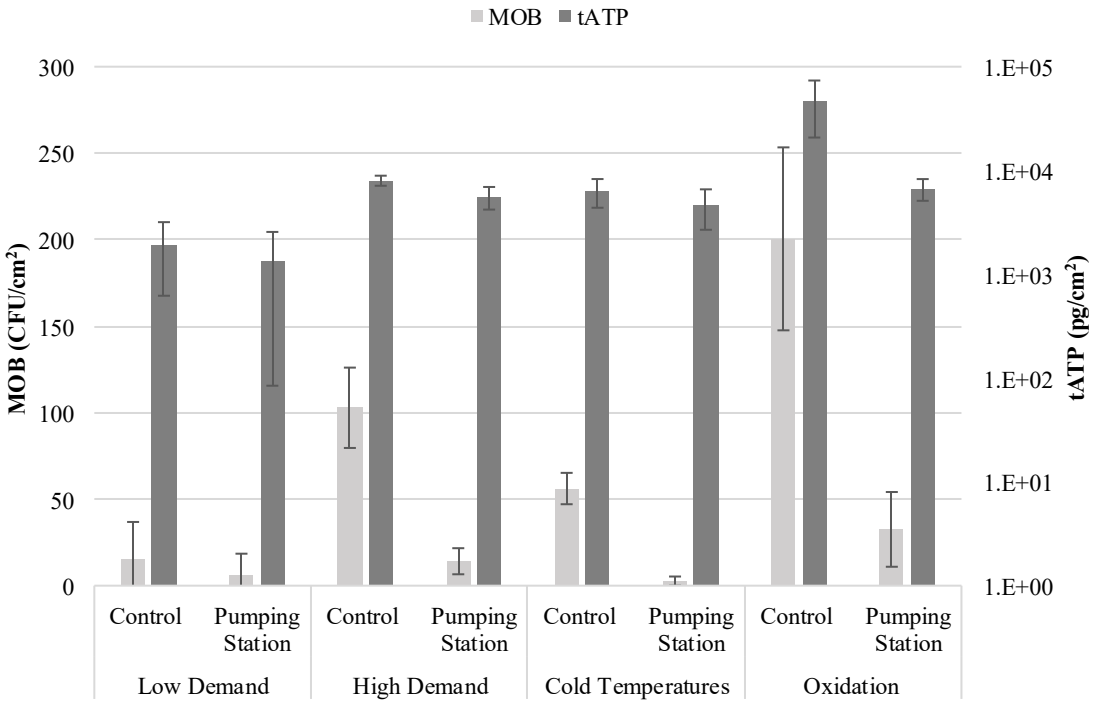

Figure 4.9 Biomass accumulation measured on the surface of the polycarbonate coupons for each experimental phase. Error bars represent the 95% confidence interval.

These results coincide with other studies that found MOB to be negatively impacted by colder water temperatures. Ginige et al. (2011) found that during cooler months, biofilm activity in distribution decreased by an order of magnitude, with Mn concentrations also decreasing significantly during this time. A case study investigating Mn removal through biofiltration found ATP concentrations to be notably lower during their cold-water experiments (Lauderdale et al., 2016); however, it should be noted their cold-water conditions were consistently above 11°C. Kohl and Medlar (2006), also found that decreased water temperature resulted in slower oxidation reactions, limiting the efficiency of Mn removal in biofilters.

Despite the adverse impact of the cold-water temperatures on biomass accumulation, Mn continued to deposit in both reactors. Mandernack et al. (1995) found that *Bacillus* strain SG-1 continued to oxidize Mn(II) onto δ-MnO_2 at temperatures as low as 3°C; therefore, MOB still active in the biofilm could potentially be oxidizing Mn in these systems. However, as seen in Figure 4.8, Mn accumulation rates remained steady between the cold temperature phase and the previous high demand phase, despite the significant decrease in MOB populations. Since the Mn accumulation rates did not decrease in response to decreasing MOB, biogenic adsorption onto previously established biofilm is likely the primary mechanism behind Mn accumulation at these temperatures.

4.3.3.3 Impact of Oxidation Enhancement on Biofilm Accumulation

Visually, as seen in Figure 4.5, oxidant enhancement resulted in an increase in biofilm accumulation and the appearance of black Mn deposits on the coupon surface. Biofilm analyses of the oxidant enhanced coupons showed that the addition of NaOCl resulted in Mn surface densities more than doubling to 6.93 $\mu g/cm^2$, in addition to the return of MOB colonies. However, these increases were not statistically significant and it is difficult to determine whether the increases were simply the result of warmer water temperatures.

A comparison of the Mn accumulation rates during this phase may provide a better insight on the effect of oxidant enhancement on Mn deposition (Figure 4.8). In the pumping station reactor, the rate of Mn accumulation increased by 89% following the addition of NaOCl. In comparison, the rate of Mn accumulation remained consistent in the control, decreasing only slightly from 0.80 $\mu g/cm^2$ per week to 0.77 $\mu g/cm^2$ per week. This large rate increase observed in the oxidant enhanced reactor suggests NaOCl contributed to increased Mn accumulation; however, the re-appearance of MOB with warmer water temperatures still may have played an important factor on Mn accumulation during this phase.

While the oxidation of Mn by chlorine has been observed in distribution (Sly et al., 1990), Mn is not easily oxidized by chlorine at a pH less than 9.5 (Brandhuber et al., 2013; Knocke et al., 1990). This is especially true in the presence of co-occurring metals such as iron, which oxidize more readily when compared to Mn. Therefore, the oxidant demand for these co-occurring metals must be fulfilled before any substantial oxidation of Mn can take place (Brandhuber et al., 2013). An EDS analysis of the coupon surfaces suggests that NaOCl may have been preferentially oxidizing iron over Mn in the pumping station reactor (Table 4.3). Following the addition of NaOCl, the average percent atomic composition of Mn increased by just 0.09%, whereas iron increased by 0.77%, nearing the percent composition of iron found on the control coupon surface.

Table 4.3 Average atomic composition (%) of the control and pumping station reactors' polycarbonate coupon surface elements obtained through EDS analysis.

	% Atomic Composition							
	C	**N**	**O**	**Al**	**Si**	**Cl**	**Mn**	**Fe**
Control	62.91	4.37	29.54	0.33	0.58	0.05	1.03	1.18
Pumping Station (Flow Increase)	86.22	0.00	13.72	0.00	0.00	0.03	0.03	0.00
Pumping Station (Post Oxidant)	82.69	0.00	16.06	0.15	0.20	0.01	0.12	0.77

4.4 CONCLUSIONS

The purpose of this chapter was to confirm manganese-biofouling of the JD Kline Water Supply Plant's raw water transmission pipe and to explore the impact of water quality and hydraulic changes on manganese and biomass accumulation. The study was performed at bench scale at the JDKWSP, using annular reactors to simulate the transmission pipe's hydraulic conditions. Reactors on either side of the transmission pipe were used to confirm manganese-biofouling, while a third reactor was run in parallel to the pumping station reactor to investigate the impact of flow rate increases, cold water conditions and oxidant enhancement on Mn-biomass accumulation. Key findings from these experiments include:

- A significant reduction in bulk water manganese was observed across the raw water transmission pipe, suggesting manganese accumulation in the system.

- Manganese accumulation across the transmission pipe was found to be statistically significant, with a final manganese surface density of 32.67 $\mu g/cm^2$ observed in the pumping station reactor and 115.93 $\mu g/cm^2$ in the pilot plant reactor.

- Acidic conditions and low bulk water manganese concentrations suggest manganese accumulation was biologically facilitated. This was confirmed by the strong Pearson correlation (ρ=0.880, P<0.0001) between manganese and MOB surface densities accumulated on the polycarbonate surfaces.

- Increased flow demand resulted in significant biofilm removal, with 4 times less manganese and 7.4 times less MOB accumulating on the coupon surface during this phase. In addition, the manganese accumulation rate was found to 5.8 times less at high demand, likely due to the higher shear stress and lower hydraulic retention time.

- Biomass was significantly reduced under the cold water conditions; however, manganese continued to accumulate in all three reactors during this time. Since manganese accumulation rates did not decrease in response to decreasing MOB, biogenic adsorption onto previously established biofilm was likely the primary accumulation mechanism.

- Manganese accumulation more than doubled to 6.93 $\mu g/cm^2$ through the addition of NaOCl as an oxidant, with accumulation rates increasing by 89% compared to the previous phase. However, it is difficult to determine whether this was simply the result warmer water temperatures, which resulted in the re-appearance of MOB colonies.

Chapter 5: IMPACT OF PHOSPHATE AND MANGANESE ON BIOFILM ACCUMULATION ONTO POLYCARBONATE SURFACES

5.1 INTRODUCTION

In relation to drinking water, Mn has long been considered an aesthetic nuisance owing to its tendency to cause water discoloration in its oxidized form. However, public health concerns regarding Mn in drinking water are rising. Not only have Mn-oxides been shown to effectively scavenge trace inorganics (Dong et al., 2003; Feng et al., 2007; McKenzie, 1980; Manceau et al., 1992; Nelson et al., 1999; O'Reilly & Hochella, 2003; Puppa et al., 2013; Wang et al., 2012; Zhao et al., 2010), but a growing number of epidemiological studies have linked Mn consumption from drinking water with neurotoxicity in school-aged children (Bhang et al., 2013; Bouchard et al., 2011; Henn et al., 2012; Khan et al., 2011; Kim et al., 2009; Shin et al., 2015). In response, Health Canada has finalized new Mn drinking water guidelines, lowering its AO from 50 to 20 µg/L and creating a MAC of 120 µg/L. With impending stricter guidelines, a better understanding of the fate of Mn in distribution is necessary.

Manganese has been shown to accumulate in distribution at concentrations well below 50 µg/L (Kohl & Medlar, 2006; Sly et al., 1990) and is facilitated by a combination of physical, chemical and biological processes (Friedman et al., 2010; Hill et al., 2010). Alkaline conditions, the presence of strong oxidants and bacterial reactions tend to accelerate the oxidation of Mn, with biological oxidation shown to be favored over abiotic processes (Hastings & Emerson, 1986; Nealson et al., 1988; Tebo, et al., 2004). The problem with Mn accumulation arises when these deposits re-enter the bulk water phase through chemical or hydraulic disturbances (Clement & Carlson, 2004; Schock et al., 2008). The release of accumulated Mn not only causes dirty water events, but can increase the concentration of the trace metals and bacteria associated with these deposits at consumer taps. While aesthetic deterioration, such as increased turbidity and colour are often markers used to identify these events, small scale releases can still result in elevated contaminant concentrations with no visible aesthetic issues (Schock, 2005).

While typically employed as a corrosion inhibitor for Pb control in distribution (Cartier et al., 2012; Kogo et al., 2017; Lytle & Schock, 1996; McNeill & Edwards, 2004; Volk at al., 2010; Woszczynski et al., 2015), phosphate can also be used to sequester bulk water Mn by delaying oxidation and preventing colloids from forming larger particles (Knocke et al., 1987; Kohl & Medlar, 2006; Sommerfield, 1999). Therefore, the presence of Mn in distribution can reduce phosphate's effectiveness as a corrosion inhibitor by exerting a competitive demand on the ions (Dalvi et al., 2015; Lytle & Snoeyink, 2002; Zhang et al., 2007). Phosphates may also have unintended consequences as a nutrient source for bacteria, enhancing bacterial cell growth in distribution (Chu et al., 2005; Jang et al., 2012; Lehtola et al., 2002; Payne, 2013; McNeill & Edwards, 2002). Increasing phosphorus has been found to cause thicker, less homogenous biofilms with increased diversity, regardless of pipe material (Fang et al., 2009; Jang et al., 2012; Payne, 2013).

Halifax Water has recently adjusted their corrosion control treatment at the JDKWSP, increasing their phosphate objective from 0.5 mg-PO_4/L to 1 mg-PO_4/L in the hopes of reducing lead corrosion in distribution. Phosphate is dosed prior to release using a zinc orthophosphate blend (Carus 3150, Carus Chemical Company, LaSalle, IL). The goal of this study is to investigate the unintended impacts of increasing phosphate doses on Mn and biomass accumulation in distribution. This study was performed at bench scale using four phosphate doses (0.7-, 1.2-, 1.7- and 2.2 mg-PO_4/L) at two Mn levels (6 µg/L and 250 µg/L).

5.2 MATERIALS AND METHODS

5.2.1 Experimental Design & Set-Up

Annular reactors were used in this study to simulate drinking water distribution at the bench scale. Four annular reactors were operated in parallel at a rotational speed of 50 rpm to achieve a shear stress of 0.25 N/m^2. This shear stress models a flow rate of 0.3 m/sec in a 100-mm diameter smooth pipe and is consistent with other studies modeling domestic plumbing systems (Gagnon et al., 2005; Garny et al., 2008; Jang et

al., 2012; Rygel, 2006; Sharp et al., 2001). Flow rates resulting in a hydraulic retention time of 2-hours were maintained, which have been shown to promote biofilm formation while minimizing planktonic growth (Camper et al., 2003; Sharp et al., 2001). Polycarbonate coupons were used to accommodate biofilm growth within the reactors, so that biofilm formation would not be influenced by corrosion products (Camper et al., 2003; Fang et al., 2009; Garny, et al., 2008; Graham et al., 2005; Rand et al., 2007; Sharp, 2001). As summarized Table 5.1, four phosphate doses at two Mn levels were investigated during this study.

Table 5.1 Summary of the experimental conditions and timeline for each annular reactor.

	Acclimation 4 weeks	**Phase 1** 8 weeks	**Acclimation** 4 Weeks	**Phase 2** 29 Weeks
AR 1	**Low Manganese** (< 6 μg/L)			
	1.7 mg-PO_4/L		0.7 mg-PO_4/L	
AR 2	**Low Manganese** (< 6 μg/L)			
	2.2 mg-PO_4/L		1.2 mg-PO_4/L	
AR 3	**High Manganese** (250 μg/L)			
	1.7 mg-PO_4/L		0.7 mg-PO_4/L	
AR 4	**High Manganese** (250 μg/L)			
	2.2 mg-PO_4/L		1.2 mg-PO_4/L	

Tap water obtained from Halifax Water was passed through a granulated activated carbon filter for chlorine removal prior to its use in this study (Figure 5.1). The reactors operating under the high Mn level were dosed with $MnSO_4$ (Fisher Scientific, ON) to obtain an influent concentration of approximately 250 µg-Mn/L, while the low Mn level reactors operated under the Mn concentrations entering through the tap water. Phosphate doses of 1.7 and 2.3 mg-PO_4/L were applied as phosphoric acid over an 8-week period at both Mn levels. Following this phase, the impact of 0.7 and 1.2 mg-PO_4/L doses were investigated over a 29-week period. Phosphate doses of 0.7 mg-PO_4/L were obtained by passing the influent water through ferric (oxyhydr)oxide filter columns to reduce phosphate concentrations. No treatment alterations were required to obtain the 1.2 mg-PO_4/L dose, as it was the average concentration of the incoming tap water.

Biofilm sampling during this phase commenced following a 4-week acclimation period between high and low phosphate doses.

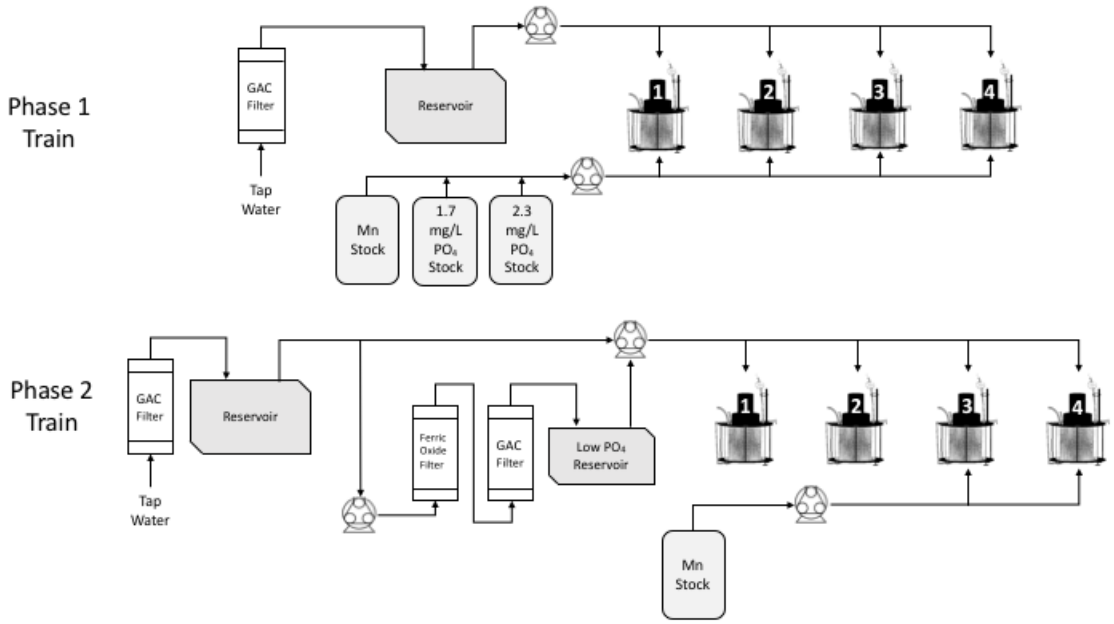

Figure 5.1 The experimental set-ups for both experimental phases. Phase 1 required the addition of phosphate, while phase 2 required the removal of phosphate through ferric (oxyhydr)oxide) filter columns.

Influent and effluent bulk water samples were collected weekly, and were analyzed for pH, temperature, turbidity, phosphate and total manganese and lead. Additional analyses of TOC, DOC and colour were performed on a bi-weekly basis. A coupon from each reactor was removed and analyzed for ATP, MOB and Mn surface densities every two weeks. Upon experimental completion, scanning electron microscopy, EDS and DNA extraction for future sequencing were also performed on the coupons. All materials and methods used during this study are described at length in Chapter 3:

5.3 RESULTS AND DISCUSSION

5.3.1 Source Water Chemistry

De-chlorinated tap water drawn from the Clean Water Lab at Dalhousie University was used as source water throughout this experiment, which ran from May 2016 to April 2017. Two Mn concentration levels and four PO_4 concentration levels were examined, requiring eight different influent waters. The average influent water quality results for each experimental condition are displayed in Table 5.2. It should be noted that DOC was unintentionally reduced at the 0.7 mg-PO_4/L dose by the ferric (oxyhydr)oxide filters used for PO_4 removal.

Table 5.2 Average influent water quality of the eight experimental conditions.

AR Conditions		Mn (µg/L)	PO_4 (mg/L)	Temp (°C)	pH	Turbidity (NTU)	DOC (mg/L)
Mn	**PO_4**						
Low	0.7-mg/L	4.08 ± 5.82	0.84 ± 0.44	21.3 ± 1.5	7.08 ± 0.41	0.13 ± 0.08	0.87 ± 0.36
	1.2-mg/L	6.67 ± 6.18	1.84 ± 0.30	20.2 ± 2.0	7.21 ± 0.17	0.21 ±0.20	1.90 ± 0.28
	1.7-mg/L	9.68 ± 10.3	1.91 ± 1.16	22.0 ± 2.1	7.34 ± 0.09	0.22 ± 0.15	2.13 ±0.46
	2.2-mg/L	8.57 ± 6.26	2.35 ± 0.87	22.0 ± 1.9	7.31 ± 0.08	0.21 ± 0.10	2.11 ±0.34
High	0.7-mg/L	214 ± 74.0	0.66 ± 0.22	21.1 ± 1.7	7.11 ± 0.36	0.18 ± 0.21	0.90 ± 0.42
	1.2-mg/L	217 ± 76.0	1.25 ± 0.31	20.2 ± 1.9	7.2 ± 0.24	0.17 ± 0.19	1.78 ± 0.22
	1.7-mg/L	208 ±20.6	1.65 ± 0.60	22.1 ± 2.1	7.43 ± 0.08	0.18 ±0.07	1.96 ± 0.21
	2.2-mg/L	180 ± 30.7	2.13 ± 0.62	21.9 ± 2.1	7.36 ± 0.08	0.17 ± 0.06	1.88 ± 0.20

5.3.2 Impact of Manganese and Phosphate on Biofilm Accumulation

A visual inspection of the polycarbonate coupons removed following 8-weeks of treatment can be seen in Figure 5.2. These images show the qualitative impact of Mn and PO_4 doses on biofilm accumulation. The accumulation of Mn appears to be greater under

the high Mn level, as indicated by the dark black-brown appearance of the biofilm. Under both Mn conditions, the biofilm appears to lighten in colour and perhaps increase in density with increasing PO_4 doses. These results suggest that PO_4 is reducing the amount of bulk water Mn being oxidized and deposited on to the coupon surfaces, which would result in lighter coloured biofilms.

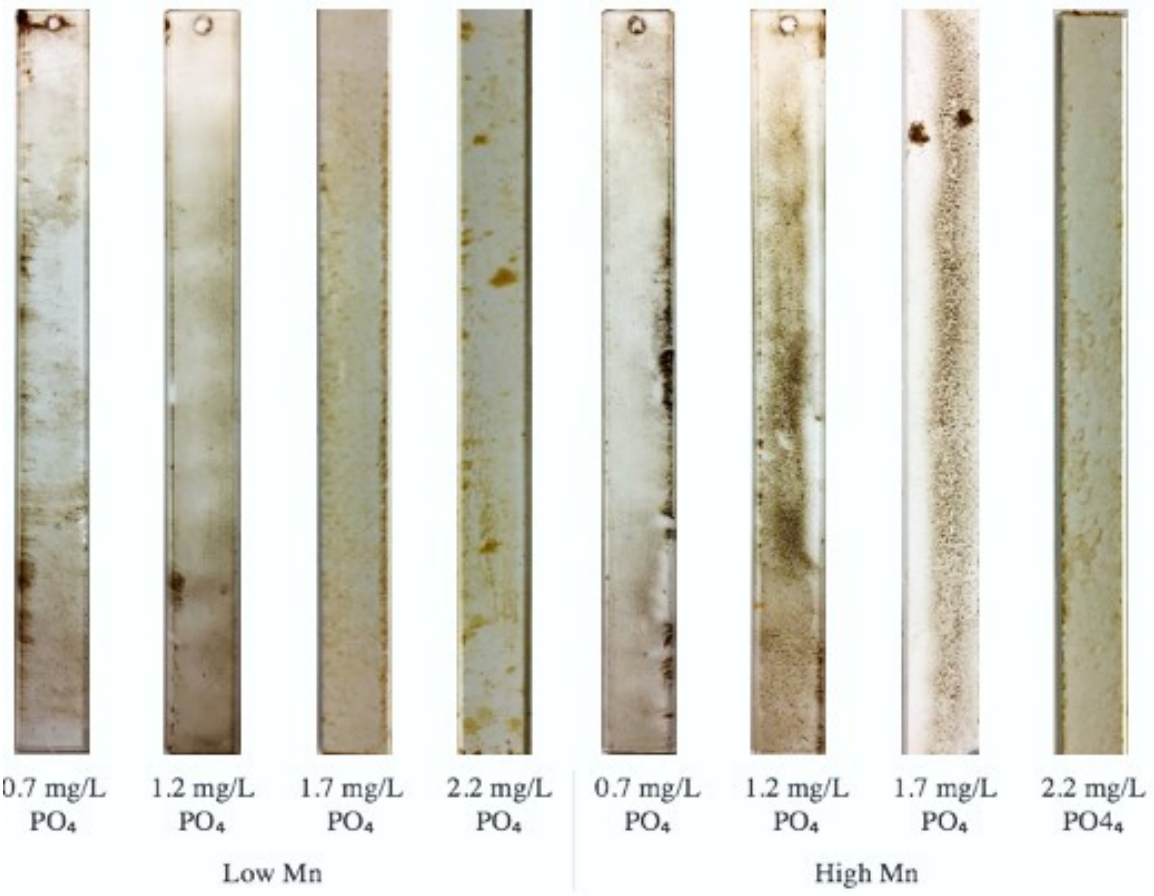

Figure 5.2 Biofilm accumulation on the polycarbonate coupons following 8-weeks of treatment under all experimental conditions.

The biofilm accumulated on the coupon surfaces were aseptically removed and analyzed for Mn, MOB and tATP surface densities on a bi-weekly basis. The Mn and MOB results are displayed in Figure 5.3, while the tATP results are shown in Figure 5.5.

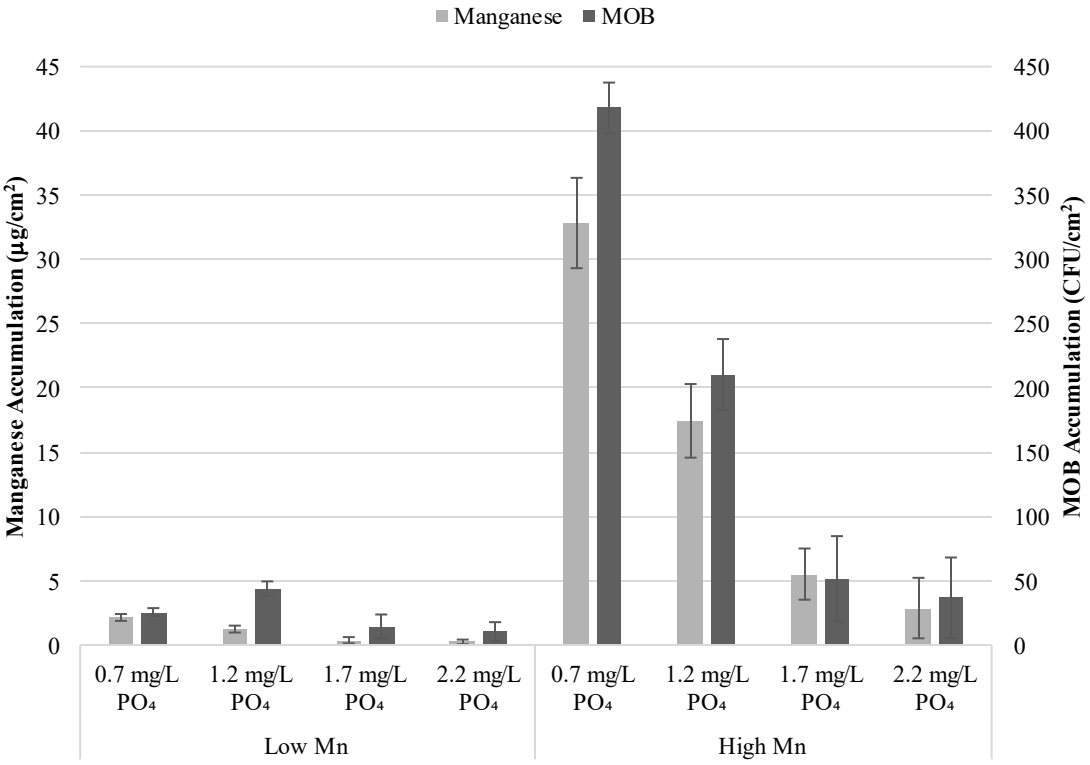

Figure 5.3 Total manganese and manganese oxidizing bacteria surface densities, measured on the polycarbonate coupons for each experimental condition. Error bars represent the 95% confidence interval.

Both Mn and PO_4 were shown to have a significant impact on Mn accumulation onto polycarbonate surfaces ($P < 0.0001$). The addition of Mn resulted in a significant increase in Mn accumulation, with a 93.5% difference observed between the two doses. In contrast, increasing PO_4 doses resulted in a significant decrease in Mn accumulation under both Mn conditions. The accumulation difference between PO_4 doses was substantial, with an 88.7% reduction observed across the low Mn condition and 91.3% reduction observed across the high Mn condition. However, there may be a limit at which PO_4 can effectively sequester Mn, as there is no significant difference in Mn accumulation following the 1.7 mg-PO_4/L dose.

These results are consistent with those found in literature, stating that Mn colloids may exert a competitive demand on phosphate ions intended for iron and Pb sequestering (Lytle & Snoeyink, 2002), and that oxidized cations such as iron and Mn show an apparent affinity to adsorb and co-precipitate with phosphate (Friedman et al., 2010).

Other studies investigating the impact of anions on metal adsorption found that the presence of phosphate significantly decreased metal accumulation onto Mn-oxides (Dalvi et al., 2015; Zhang et al., 2007). Zhang et al. (2007) for example, determined that over the other anions studied, PO_4 caused the largest interference on arsenic adsorption onto Fe-Mn oxides, likely due to the competitive sorption brought on by phosphate ions. Similar results with cations were obtained by Payne (2013) who found that the addition of PO_4 resulted in a decrease in Pb adsorption onto polycarbonate surfaces.

The biofilm accumulated on the coupon surfaces at the 0.7 and 1.2 mg-PO_4/L conditions were analyzed by EDS (Table 5.3). The results corroborate the Mn biofilm results, showing that the coupon surface was composed of 1.42% Mn by weight under the high Mn, 0.7 mg-PO_4/L dose and only to 0.63% Mn at the 1.2 mg-PO_4/L dose. Under the low Mn conditions, the coupon surface contained less than 0.1% Mn by weight. A study investigating Mn accumulation onto PVC pipes obtained similar results, finding that the pipe scale formed by water containing 282 µg-Mn/L was comprised of 6.12% Mn by weight (Cerrato et al., 2005). The EDS analysis also showed that the biofilms contained more phosphorus by weight under the 1.2 mg-PO_4/L condition. This indicates PO_4 may have been forming passivating scales at the higher doses, resulting in less Mn accumulation.

Table 5.3 Average atomic composition (%) of the polycarbonate coupon surface elements obtained through EDS analysis for the 0.7 and 1.2 mg-PO_4/L doses.

		% Atomic Composition							
Condition		**C**	**N**	**O**	**Al**	**P**	**Ca**	**Mn**	**Fe**
Low Mn	0.7 mg/L PO_4	79.56	0.00	19.75	0.19	0.09	0.01	0.07	0.33
	1.2 mg/L PO_4	83.75	1.21	14.66	0.05	0.22	0.00	0.03	0.07
High Mn	0.7 mg/L PO_4	81.76	0.00	16.19	0.04	0.03	0.00	1.42	0.57
	1.2 mg/L PO_4	65.77	1.22	27.56	3.05	0.35	0.18	0.63	1.25

The accumulation of MOB was also shown to be significantly impacted by both Mn and PO_4 concentrations ($P < 0.001$). As seen in Figure 5.3, the addition of Mn resulted in a significant increase in MOB surface densities, with the bacteria appearing to be more productive in oxidizing Mn under the high Mn condition. Increasing PO_4 dose resulted in a decrease in MOB; however, this difference was determined to be insignificant between the two highest doses. As seen in Figure 5.4, Mn and MOB were found to be significantly correlated in the biofilm, with a Pearson correlation coefficient of 0.957, ($P < 0.0001$). This strong correlation suggests MOB are facilitating the oxidation of Mn onto the coupon surfaces. Clustered results from the various PO_4 and Mn doses further proves their significant impact on Mn-biofilm formation. Similar results were obtained by Ginige et al. (2011) that found a significant positive correlation between biofilm activity and Mn deposition onto glass surfaces.

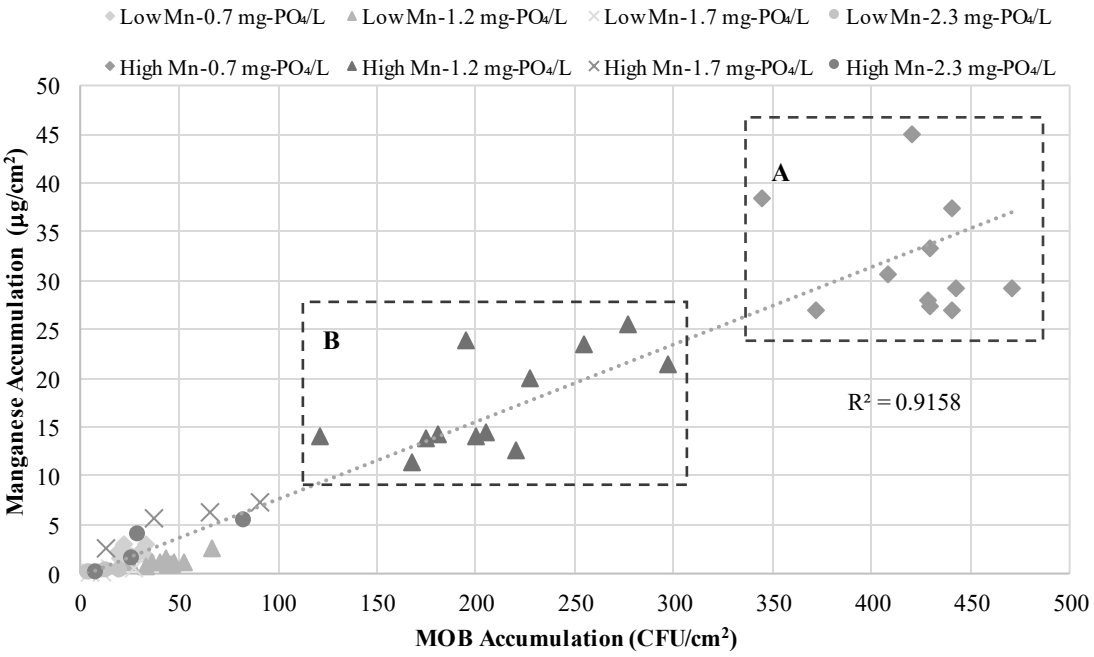

Figure 5.4 Matched data points for manganese densities and plate counted manganese oxidizing bacteria measured on the polycarbonate coupon surfaces. Drawn boxes indicate major trends from the experimental conditions. Box A denotes the high manganese and 0.7 mg-PO_4/L dose results, while box B denotes high manganese and 1.2 mg-PO_4/L dose results.

Biofilm tATP was also measured over the course of the experiment as a secondary assessment of microbial population. Results in Figure 5.5 show tATP surface densities increasing in response to the addition of PO_4. Both PO_4 and Mn proved to have a statistically significant impact on tATP accumulation ($P < 0.0001$); however, tATP was only significantly different following the 0.7 mg-PO_4/L dose. While these results are in contrast with the trends observed with the MOB and Mn surface densities, they coincide with the results obtained by Payne (2013), who observed increasing ATP microbial activity at higher phosphate doses. Other studies observed a similar trend with heterotrophic plate counts, where the number of colonies increased with the addition of phosphorus (Chu et al., 2005; Fang et al., 2009; Jang et al., 2012; Payne, 2013).

These results indicate that phosphate is likely acting as a nutrient source, resulting in increased microbial populations. As a bacterial nutrient, phosphorus would likely lead to the preferential growth of heterotrophic bacteria, as MOB have been shown to grow at a much slower rate (Rygel, 2006). The preferential growth of faster growing bacteria would explain how tATP activity increased with PO_4 dose, despite the decrease in MOB populations. The sequestering of Mn by phosphate would also result in a similar outcome. By sequestering Mn, the amount available to MOB is reduced, which could result in heterotrophic bacteria out-competing MOB within the biofilm. In either case, phosphate being used as a nutrient source or as a sequestering agent could be limiting its efficacy in its intended role as a corrosion inhibitor.

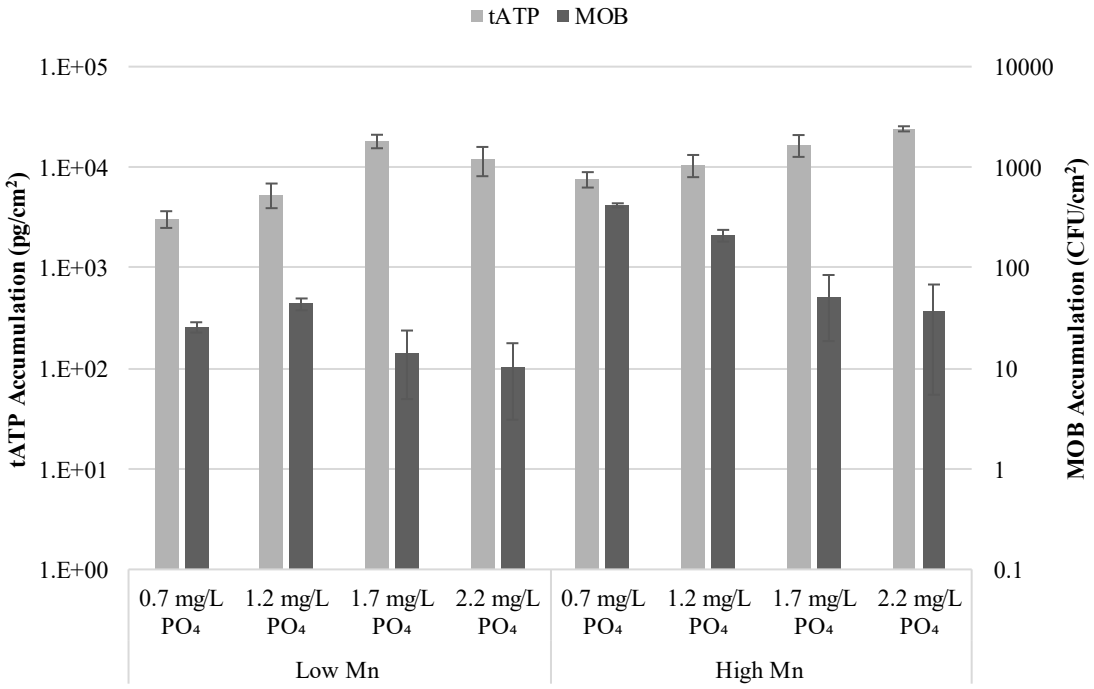

Figure 5.5 Biomass accumulation, measured on the surface of the polycarbonate coupons for each experimental condition. Error bars represent the 95% confidence interval.

5.3.3 Proposed Role of Phosphate on Manganese and Biofilm Formation

The results obtained from biofilm analysis suggests PO_4 performs two mechanisms under the investigated conditions, Mn sequestering and bacterial growth through nutrient enhancement. As illustrated in Figure 5.6 B, the addition of PO_4 allows for the formation of manganese-orthophosphate compounds, which prevent bulk water Mn from being chemically oxidized (Heinzte, 1968; Knocke et al., 1987; Kohl & Medlar, 2006; Sommerfield, 1999), allowing them to pass through the system. Manganese-orthophosphate compounds may also limit the bioavailability of Mn(II) for MOB oxidation, further reducing Mn accumulation in the biofilms. The role of PO_4 as a nutrient source would explain how the addition of PO_4 resulted in increased microbial populations, despite the decrease in MOB. As illustrated in Figure 5.6 B, the addition of PO_4 could result in the preferential growth of heterotrophic bacteria, which would out-compete the slower growing MOB within the biofilm (Rygel, 2006).

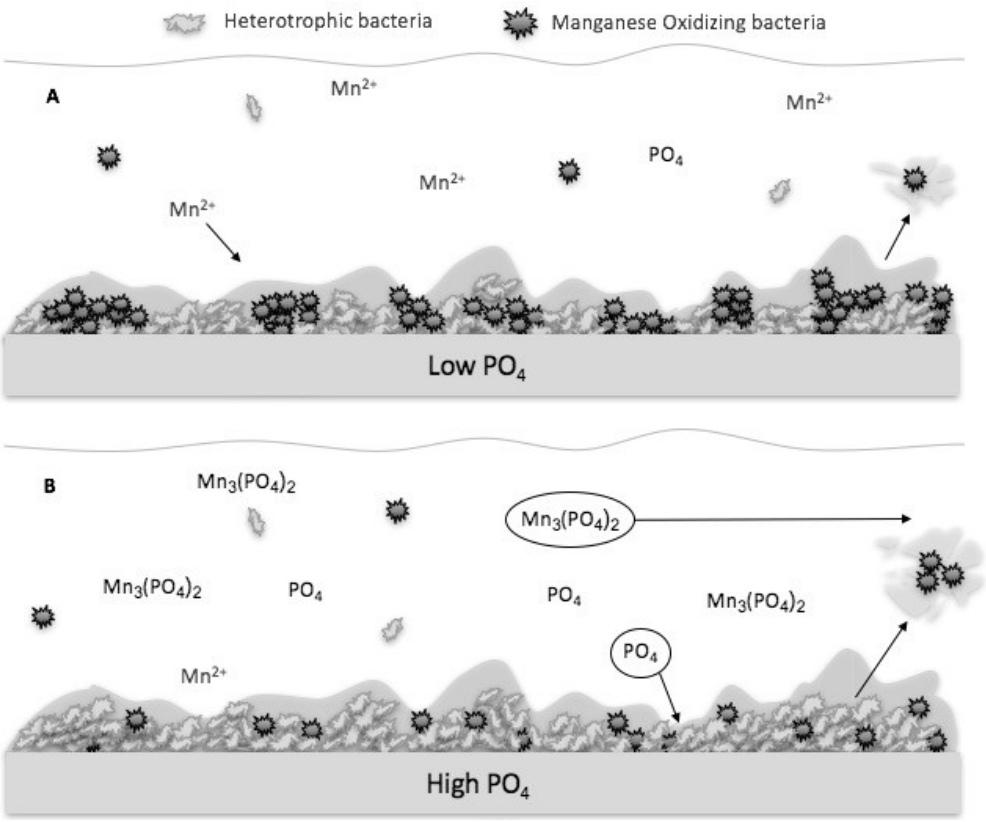

Figure 5.6 Conceptual drawing of the effect of low phosphate (A) and high phosphate (B) doses on bulk water manganese and the formation of biofilm.

The proposed roles of PO_4 in these systems as a sequestering agent and as a bacterial nutrient source, are not mutually exclusive. However, they both lead to the same outcomes for biofilm formation: a decrease in Mn accumulation and an increase in microbial population.

5.3.3.1 Removal of Bulk Water Manganese

In response to the biofilm results and the proposed role of PO_4 as a sequestering agent, the removal of Mn from the bulk water phase was expected to decrease with increasing PO_4 dose. However, as seen Figure 5.7, the opposite trend was observed, where a greater amount of Mn was removed at the higher PO_4 doses. Considering the increase in bulk water Mn removal did not correspond with an increase in Mn accumulation on the coupon surfaces, there must be Mn that was unaccounted for within the systems.

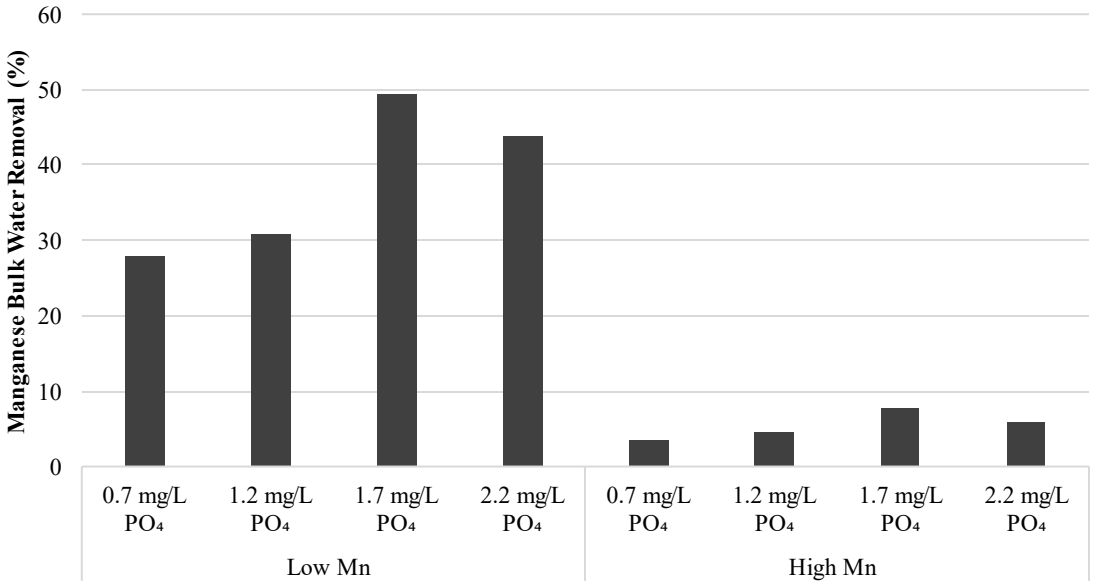

Figure 5.7 Estimated percent of manganese removed from the bulk water phase for each experimental condition.

By estimating the total mass of Mn entering and leaving the reactors, as well as the amount accumulated on the coupon surfaces, a Mn mass balance for each experimental condition could be calculated. The results shown in Figure 5.8 confirm a substantial Mn discrepancy within each system, suggesting Mn concentrations were underestimated either in the bulk water phase or within the accumulated biofilm. Unaccounted for Mn was found to increase with PO_4 dose and was more pronounced under the high Mn condition. These results could be explained by the association of Mn and PO_4 in the effluent waters, which may have resulted in the need for nitric acid digestion to recover representative Mn concentrations.

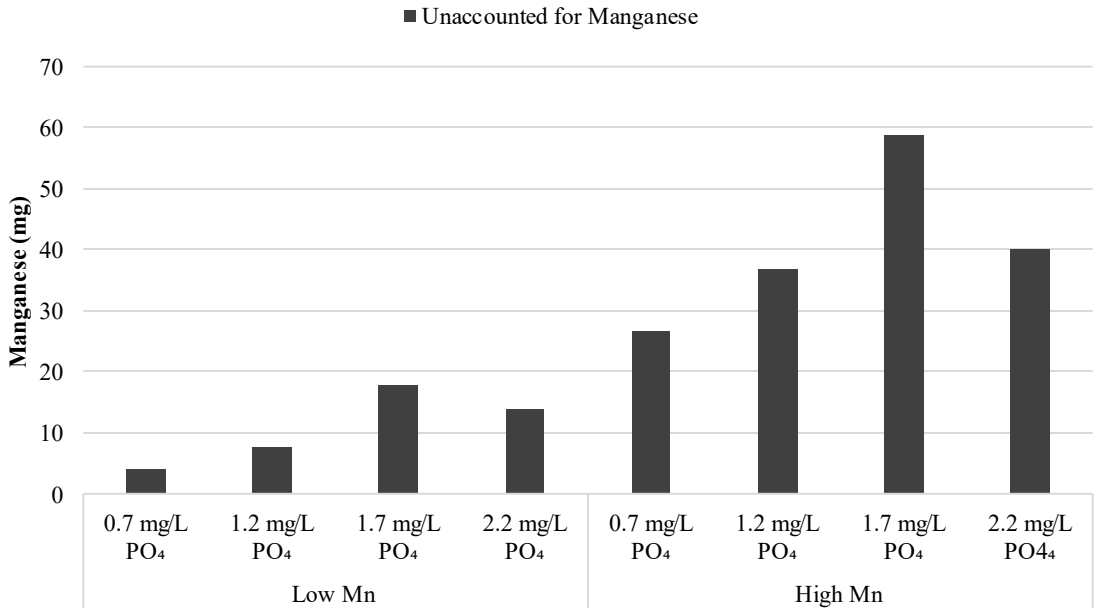

Figure 5.8 Estimated mass of unaccounted for manganese for each experimental condition, calculated through system mass balances.

5.3.3.2 Comparison of Nitric Acid Preservation and Nitric Acid Digestion

While effluent turbidity never exceeded 1 NTU, the threshold in which nitric acid digestion is required by Standard Methods 3030E (APHA, 2012), the use of nitric acid preservation was suspected to be inadequate in recovering representative Mn concentrations during metal analysis. To confirm, a comparison of the two methods was conducted at the 0.7 and 1.2 mg-PO_4/L doses, to determine if nitric heat digestion resulted in Mn concentrations that were statistically different. These results, along with the average sample turbidity are summarized in Table 5.4.

Table 5.4 Comparison of average manganese concentrations measured from nitric acid preservation and nitric acid digestion methods.

Experimental Conditions		Turbidity (NTU)	Nitric Preservation (µg/L)	Nitric Heat Digestion (µg/L)	Paired T-Test P-Value
Low Mn	0.7 mg/L PO_4	0.432	3.96 ± 0.44	5.03 ± 0.66	0.046
Low Mn	1.2 mg/L PO_4	0.285	5.60 ± 1.33	8.43 ± 1.80	0.012
High Mn	0.7 mg/L PO_4	0.351	160.17 ± 1.92	164.01 ± 2.90	0.039
High Mn	1.2 mg/L PO_4	0.158	155.93 ± 2.90	160.87 ± 4.29	0.022

Under all experimental conditions, paired t-tests showed that Mn concentrations increased significantly with use of nitric acid heat digestion. This confirms that despite turbidity being well below 1 NTU throughout the experiment, nitric acid digestion was required to obtain representative Mn concentrations in the effluent waters. These results are consistent with the findings of others (Payne, 2013; Triantifyllidou et al., 2007), who demonstrated particulate lead was significantly underestimated by nitric acid preservation, regardless of turbidity.

To account for the underestimation of Mn in the effluent waters, an adjustment factor was calculated by dividing the nitric acid digestion and nitric acid preservation results. This factor was then applied to the Mn mass balance calculations. The results, displayed in Figure 5.9, show that the adjustments substantially reduced the amount of unaccounted for Mn in the systems. For example, following the adjustment, a 75% decrease in unaccounted for Mn was observed under the high Mn, 1.2 mg- PO_4 /L experimental condition. This supports the idea that effluent waters required nitric acid digestion for analysis and should be considered for all future Mn analyses, regardless of the sample's turbidity.

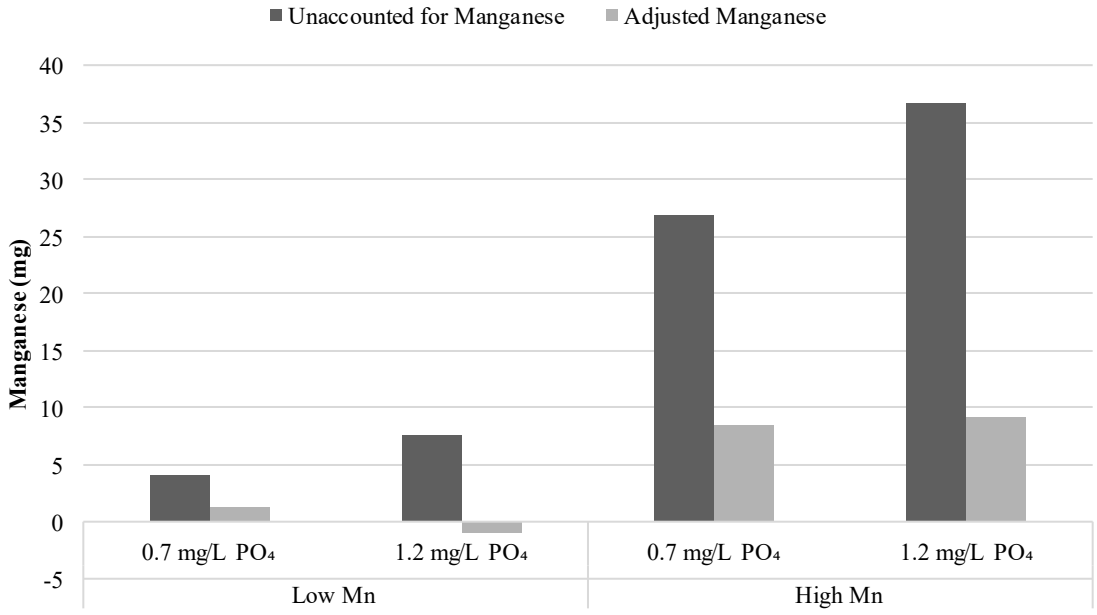

Figure 5.9 Unaccounted for manganese and adjusted manganese mass balances, comparing nitric acid preservation and nitric acid digestion methods.

5.4 Conclusions

The objective of this chapter was to investigate the impact of phosphate and manganese doses on the accumulation of manganese and biomass onto polycarbonate surfaces. This work was conducted at the bench scale using annular reactors to simulate distribution. The impacts of four phosphate doses (0.7, 1.2, 1.7 and 2.2 mg-PO_4/L) at two manganese levels (< 6 μg/L and 250 μg/L) were investigated during this study. The main findings of this work include:

- The addition of manganese resulted in a significant increase in manganese accumulation onto polycarbonate surfaces, while increasing phosphate doses resulted in a significant decrease in manganese accumulation.

- Manganese and manganese oxidizing bacteria were found to be strongly correlated within the biofilm ($\rho = 0.957$, $P<0.0001$), suggesting the oxidation of manganese was biologically facilitated.

- Biofilm microbial populations were shown to increase with increasing phosphate dose, confirming its role as a nutrient source.

- Results suggest PO_4 is acting as a sequestering agent, reducing bulk water manganese oxidation, as well as acting as a nutrient source, allowing for the preferential growth of heterotrophic bacteria, which out-compete the slow growing manganese oxidizing bacteria within the biofilm.

- Increased manganese removal from the bulk water phase did not correspond with an increase in manganese accumulation onto the polycarbonate surfaces, suggesting manganese was being underestimated somewhere within the system.

- A comparison of nitric acid preservation and nitric acid digestion determined effluent manganese was being significantly underestimated by nitric acid preservation, resulting in unaccounted for manganese in the effluent bulk water.

Chapter 6: IMPACT OF RESIDUAL PHOSPHATE AND MANGANESE ON DOWSTREAM LEAD PIPES

6.1 INTRODUCTION

Historically, lead was a common component in drinking water systems and was used in lead service lines, lead-tin solder and brass faucets. While the use of lead service lines has been banned since 1975 and lead solder since 1990 in Canada (Health Canada, 2009), previously installed leaded components are still of public health concern in older buildings. The release of lead into drinking water occurs through the dissolution of leaded materials, and is influenced by the age of the service line or fixture, stagnation times and the water quality within the system. The presence of lead in domestic plumbing poses a significant risk to public health, as lead consumption, even at low concentrations, has been shown to cause neurological deficiencies in school-aged children (Evens, et al., 2015).

Phosphate based corrosion control treatments are commonly used in drinking water systems, with 56% of American water utilities reporting its application for corrosion control in 2001 (McNeill & Edwards, 2002). Phosphates effectively reduce lead release in distribution (Kogo et al., 2017; Lytle & Schock, 1996; Woszczynski et al., 2015), by forming protective insoluble scales, which passivate the surface of the pipe (Schock, 1989; USEPA, 2011). However, phosphate has been shown to interact with other constituents in the water, limiting its efficacy as a corrosion inhibitor. For example, phosphorus is an essential nutrient in bacterial growth, and has been shown to increase microbial populations in biofilms (Chu et al., 2005; Jang et al., 2012; Lehtola et al., 2002; Payne, 2013; McNeill & Edwards, 2002).

While typically employed for Pb control, phosphates can also be applied to sequester Mn in distribution. Sequestering prevents the oxidation of Mn and inhibits colloids from forming larger particles (Knocke et al., 1987; Kohl & Medlar, 2006; Sommerfield, 1999). Therefore, the presence of Mn in distribution may exert a competitive demand on the phosphate ions, reducing its availability for corrosion control (Dalvi et al., 2015; Lytle &

Snoeyink, 2002; Zhang et al., 2007). Lead has been shown to have a preferred association with Mn-oxides over a variety of heavy metal and oxide substrate combinations (Feng et al., 2007; Manceau et al., 1992; McKenzie, 1980; O'Reilly & Hochella, 2003; Puppa et al., 2013; Wang et al., 2012); leading to the mobilization of lead in distribution. A recent study by Schock et al. (2014) suggested that the presence of Mn obstructs the formation of insoluble Pb(IV) scales, resulting in increased lead dissolution in distribution.

The relationship between Pb and Mn in distribution is still largely unknown, and is even more obscured in the presence of phosphates. With the implementation of new drinking water guidelines on the horizon, a better understanding of Mn interactions in distribution is necessary. The purpose of this study is to investigate the downstream impacts of residual phosphate and manganese on stagnated and flowing water in lead pipes. This study was performed at bench scale, using the effluent waters from the annular reactors in operation for the Chapter 5: experiments. The impact of two phosphate doses (0.7 and 1.2 mg-PO_4/L) at two Mn levels (< 6 µg/L and 250 µg/L) were investigated during this study.

6.2 MATERIALS AND METHODS

6.2.1 Experimental Design & Set-Up

To investigate the downstream impacts of residual phosphate and manganese on lead pipes, discharge from the annular reactors in operation for the Chapter 5: study, were fed directly into lead pipe sections (Figure 6.1). Four harvested lead pipes from a lead service line replacement in Halifax, Nova Scotia were soaked in 10% nitric acid solution to remove pre-existing pipe scale. The pipe sections were then directly fed effluent water from the annular reactors and allowed to acclimate over a four-month period to ensure metal stabilization (Knowles et al., 2015). Four of the 8 experimental conditions investigated in Chapter 5: were examined under both flowing and stagnant conditions, two phosphate doses (0.7 mg-PO_4/L and 1.2 mg-PO_4/L) at two Mn levels (< 6 µg/L and 250 µg/L).

Figure 6.1 The harvested lead-pipe sections (A), and the experimental set-up, with annular reactor discharge being fed into the lead-pipe sections (B).

Following the conditioning period, flowing water samples were collected weekly and analyzed for pH, temperature, turbidity, phosphate, manganese and lead. The pipe sections were then filled and stagnated for a 6-hour period, which is the stagnation period recommended by Health Canada prior to lead sampling. Stagnated samples were analyzed for pH, temperature, turbidity, TOC, phosphate, manganese and lead. At the end of the experimental period, the pipes were filled and shaken at 200 RPM for 24 hours to dislodge any formed scales. These samples were then pelleted for DNA extractions and future sequencing. A full description of methods and materials are outlined in Chapter 3:

6.3 RESULTS AND DISCUSSION

6.3.1 Source Water Chemistry

To investigate the impact of residual PO_4 and Mn on downstream Pb-pipes, discharge from Chapter 5:'s annular reactors were fed directly into Pb-pipe sections. As a four-month acclimation period was required to condition the Pb-pipes, only four of the eight experimental conditions studied in Chapter 5: could be investigated during this study, which ran from September 2017 to April 2017. The average water quality for each experimental condition is summarized in Table 6.1. There is a statistically significant difference in DOC observed between PO_4 doses due to the unintentional removal of DOC by the ferric (oxyhydr)oxide filter columns used to reduce PO_4 concentrations.

Table 6.1 Average lead pipe influent water quality for each experimental condition.

Condition		Mn	PO_4	Pb	Temp	pH	Turbidity	DOC
Mn	**PO_4**	(µg/L)	(mg/L)	(µg/L)	(°C)		(NTU)	(mg/L)
Low	0.7-mg/L	2.94 ± 1.84	0.55 ± 0.25	58.5 ± 45	20.9 ± 1.5	7.00 ± 0.39	0.65 ± 0.16	0.83 ± 0.40
	1.2-mg/L	4.61 ± 4.18	1.29 ± 0.30	35.4 ± 30	20.5 ± 1.5	7.20 ± 0.17	0.33 ±0.19	1.79 ± 0.25
High	0.7-mg/L	207.3 ± 70.2	0.61 ± 0.28	35.6 ± 61	21.0 ± 1.4	7.00 ± 0.36	0.37 ± 0.25	0.84 ± 0.39
	1.2-mg/L	207.8 ± 68.4	1.27 ± 0.32	16.6 ± 16	20.7 ± 11.5	7.16 ± 0.18	0.23 ± 0.12	1.51 ± 0.45

6.3.2 Impact of residual manganese and phosphate on flowing water in lead pipes

Over the course of the experiment, flowing water samples were collected from the Pb-pipe sections and was analyzed for both Mn and Pb. Incoming Pb was found to represent a small fraction of the total Pb measured in the effluent bulk water (1.4 – 6.7%), whereas incoming Mn represented a substantial amount of the Mn measured in the effluent (41.2 – 88.2%). This implies that most the Pb measured in the effluent bulk water was the result of Pb-release, while much of the effluent Mn originated from the influent water. Figure 6.2 shows the evolution of effluent Mn and Pb over the experimental period under the most extreme condition: 6-hour stagnation period, at the high Mn level and 1.2 mg-PO_4/L dose. These results follow the same general trend of the other experimental

conditions, where bulk water Mn concentrations increased over time, while bulk water Pb concentrations decreased over time, possibly due to the formation of passivated scales (Schock, 1989).

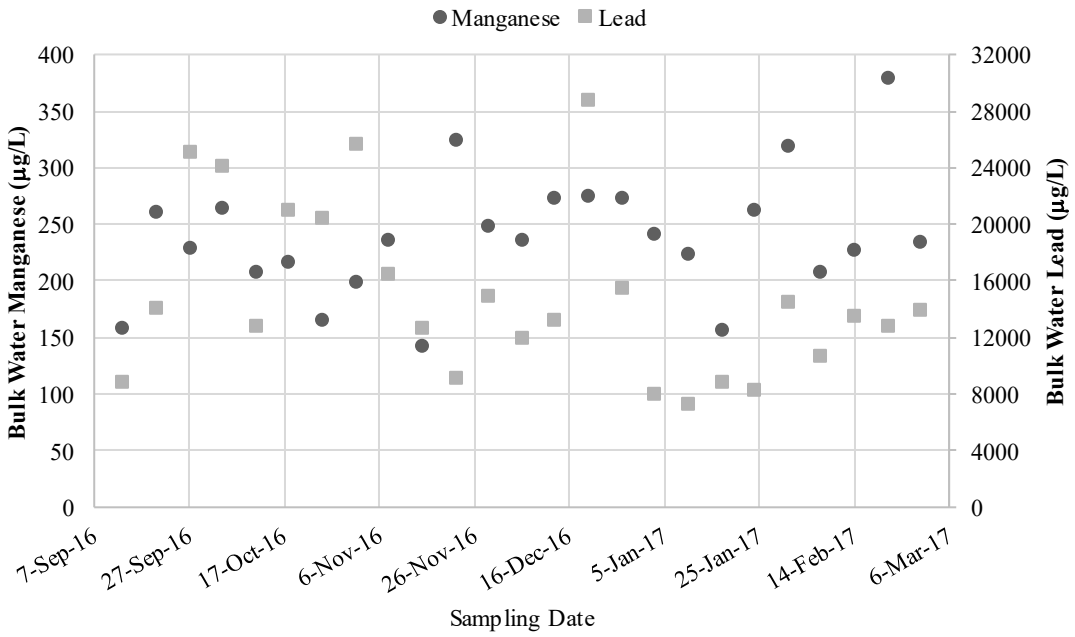

Figure 6.2 The evolution of effluent manganese and lead over the experimental period measured under the 6-hour stagnation, high manganese, 1.2 mg-PO_4 condition.

The bulk water results for all of the experimental conditions are summarized in boxplots, as the data was not found to be normally distributed under many of the experimental conditions (Figure 6.3)

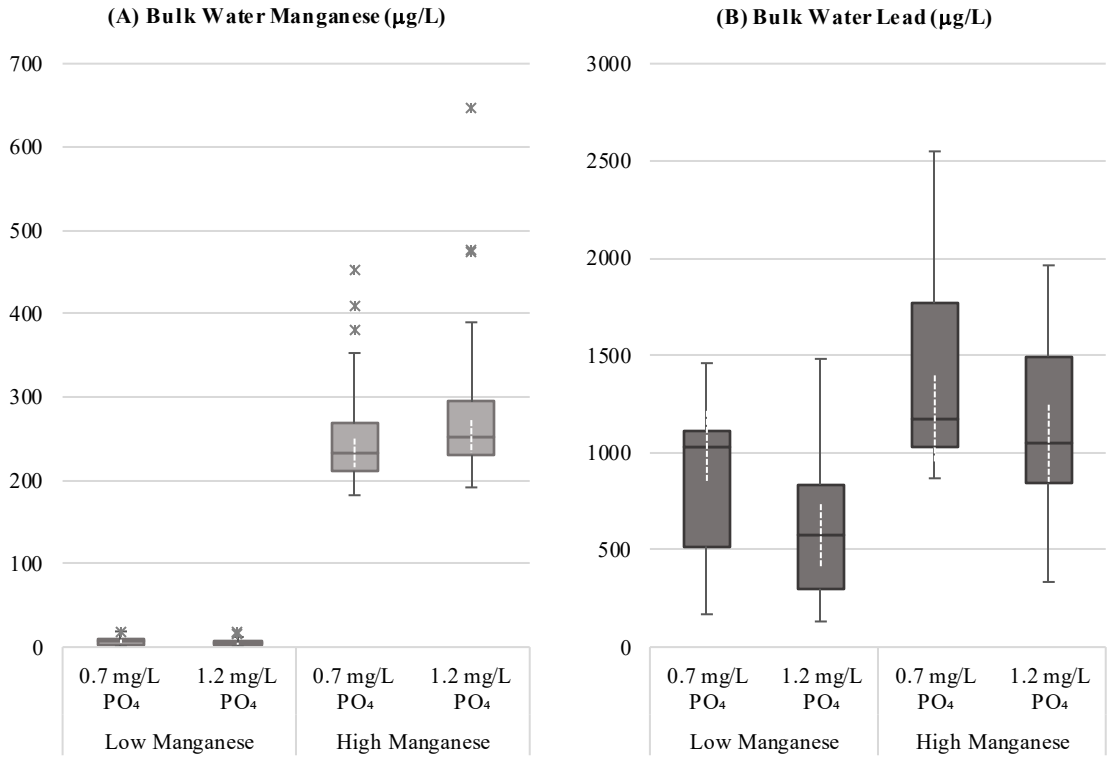

Figure 6.3 Distribution of (A) bulk water manganese concentrations and (B) bulk water lead concentrations for each flowing water experimental condition. In each box plot, the median value is indicated by the horizontal line, outliers by asterisks and the 95% confidence interval by the dashed line. In the presence of outliers, vertical lines represent 1.5 times the interquartile range, otherwise they indicate minimum and maximum values.

As seen in Figure 6.3 B, the addition of Mn resulted in an increase in bulk water Pb concentrations. A comparison of the medians show that the effect of Mn was more pronounced at the 1.2 mg-PO_4/L level, with Pb concentrations increasing by 83.1% across the 1.2 mg-PO_4/L dose and by only 13.4% across the 0.7 mg-PO_4/L dose. To assist in statistically comparing the medians, 95% confidence intervals were calculated using an equation outlined by McGill, Tukey and Larsen (1978): median $\pm$ 1.58 x IQR / $\sqrt{n}$. The confidence interval results indicated that the increase in bulk water Pb due to the addition of Mn was only significant at the 1.2 mg-PO_4/L dose.

The increase in Pb release suggests Mn particles are mobilizing Pb into the bulk water phase. Trueman & Gagnon (2016) determined that iron rich colloidal particles were

mobilizing Pb through strongly correlated elution profiles. Since Pb has shown a preferred association with Mn over all other heavy metal and oxide substrate combinations (Feng et al., 2007; Manceau et al., 1992; McKenzie, 1980; O'Reilly & Hochella, 2003; Puppa et al., 2013; Wang et al., 2012), it is likely that Mn particles can mobilize Pb in distribution as well. Mn could also be obstructing the formation of insoluble Pb(IV) scales, which would result in an increase in Pb dissolution, as suggested by Schock et al. (2014).

While PO_4 was shown to have no meaningful impact on bulk water Mn concentrations (Figure 6.3 A), it was shown to decrease Pb-release under both Mn conditions. Under the low Mn condition, PO_4 significantly reduced the median Pb concentrations by 80.1%. At the high Mn level, the difference in bulk water Pb concentrations was found to be insignificant, decreasing by only 11.9% with the addition of PO_4. These results are consistent with other studies that found Pb release in premise plumbing was significantly reduced through the addition of PO_4 (Kogo et al, 2017; Lytle & Schock, 1996; Woszczynski et al., 2013). Furthermore, Trueman et al. (2017) demonstrated that PO_4 reduces Pb release in iron-lead galvanic systems; however, in the presence of interfering agents such as natural organic matter, PO_4 becomes less effective as a corrosion control inhibitor. The additional PO_4 likely increased the Pb-pipe surface's passivity by forming a less soluble surface, preventing Pb dissolution into the bulk water phase (Schock, 1989). The lower effectiveness of PO_4 at the high Mn concentration suggests that Mn is interacting with PO_4; therefore, reducing its ability to passivate the Pb-pipe surfaces.

6.3.3 Impact of residual manganese and phosphate on stagnated lead pipes

To investigate the impact of Mn and PO_4 on stagnated Pb-pipes, bulk water Mn and Pb concentrations were measured following a 6-hour stagnation period (Figure 6.4).

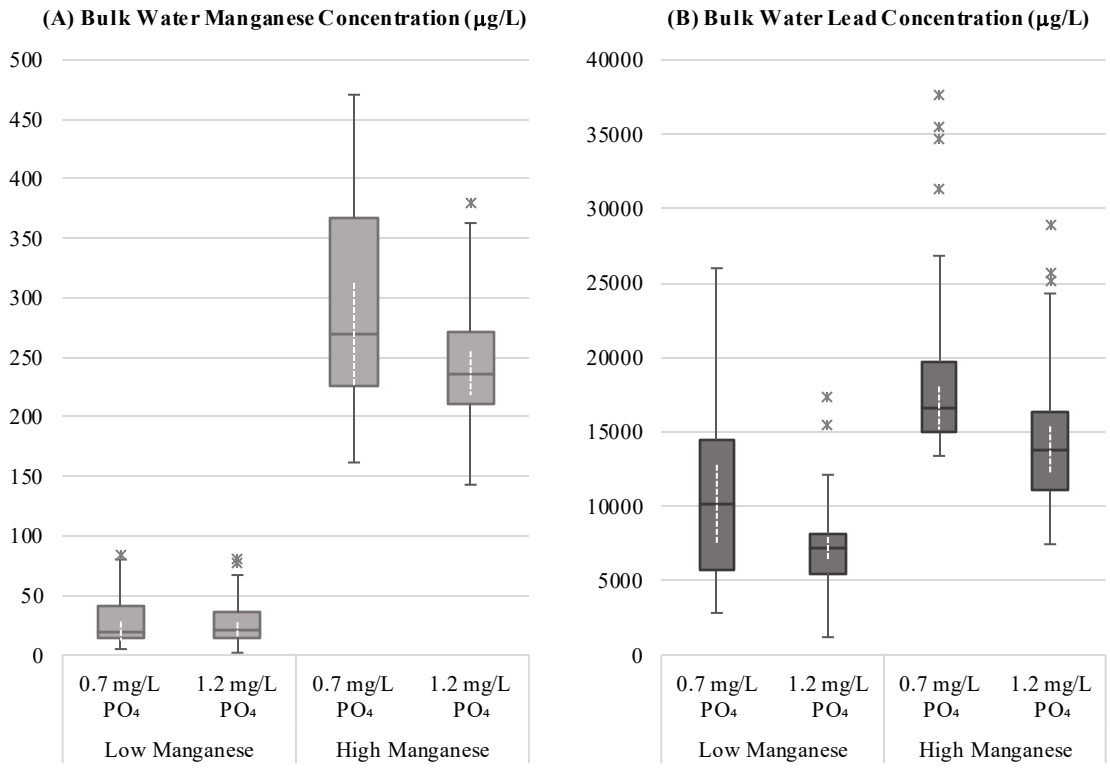

Figure 6.4 Distribution of (A) bulk water manganese concentrations and (B) bulk water lead concentrations for each 6-hour stagnation experimental condition. Median values are indicated by horizontal lines, outliers by asterisks, and the 95% confidence intervals by dashed lines. In the presence of outliers, vertical lines represent 1.5 times the interquartile range, otherwise they indicate minimum and maximum values.

Following stagnation, bulk water Mn concentrations were only found to be significantly different at the low Mn dose ($P < 0.0001$). Bulk water Pb on the other hand, significantly increased under all experimental conditions following stagnation. Several studies have found Pb-release to significantly increase following stagnation periods. Lytle and Schock (2000) determined Pb release increased exponentially over a 90-hour stagnation period, with 50-70% of Pb being released in the first 10-hours. Woszczynski et al. (2015) also found Pb release to be significantly higher following a 24-hour stagnation period. While Kogo et al. (2017) found Pb-release increased significantly following a 6-hour stagnation period, the increase in Pb-release was found to be insignificant in the presence of orthophosphate.

Aesthetically, effluent water deteriorated significantly following the 6-hour stagnation period, as seen in Figure 6.5. While turbidity increased significantly in the flowing water discharge, turbidity and colour increased dramatically following stagnation (Table 6.2). The turbidity measured from the stagnated water increased by over an order of magnitude, with large lead particles being visually detectable in the bulk water. This decline in aesthetic water quality with increasing lead concentrations corroborates the findings of Pieper et al. (2017), who concluded that increasing water discoloration was predictive of high lead levels in a residence in Flint, Michigan.

Figure 6.5 Turbidity samples measured from (A) the flowing pipe discharge and (B) the 6-hour stagnation period obtained under the low manganese, 0.7 mg-PO_4/L experimental condition.

Table 6.2 Average turbidity and bulk water lead concentrations for each experimental condition sampled from the flowing water effluent and following the 6-hour stagnation.

Condition		**Turbidity (NTU)**			**Lead Concentrations (µ/L)**	
Mn	PO_4	Influent	Flowing Water	6-hour stagnation	Flowing Water	6-hour stagnation
Low	0.7-mg/L	0.65 ± 0.16	1.74 ± 1.4	20.5 ± 13.2	869 ±381	10982 ± 6097
	1.2-mg/L	0.33 ± 0.19	1.58 ± 1.6	22.9 ± 8.7	601 ± 388	7246 ± 3558
High	0.7-mg/L	0.37 ± 0.25	2.55 ± 2.6	27.3 ± 10.8	1421 ± 539	19308 ± 7077
	1.2-mg/L	0.23 ± 0.12	2.65 ± 2.0	29.1 ± 13.4	1147 ± 462	14943 ± 5904

As shown in Figure 6.4, similar trends observed during the flowing conditions were observed following the stagnation period. Based on the 95% confidence intervals, the addition of Mn significantly increased bulk water Pb concentrations at both PO_4 levels, with Pb release increasing by 64.3% at the 0.7 mg-PO_4/L dose and by 93.2% at the 1.2 mg-PO_4/L dose. Under both Mn conditions, PO_4 was shown to decrease Pb-release; however, the reduction was not found to be significant at either level. Comparing the median Pb concentrations, PO_4 was shown to be less effective in reducing bulk water Pb concentrations at the high Mn dose. Under the low Mn condition, PO_4 reduced Pb-release by 41.8%, while only reducing it by 20.7% under the high Mn condition. These results further indicate that Mn is obstructing the formation of insoluble Pb scales, increasing Pb dissolution into the bulk water phase. The addition PO_4 was shown to have no significant impact on bulk water Mn concentrations.

6.4 Conclusions

The focus of this chapter was to study the downstream impacts of residual phosphate and manganese on stagnated and flowing water in lead pipes. This experiment was performed at bench scale using clean lead pipe sections, using the annular reactor effluent from Chapter 5:'s experiments as the source water. The effect phosphate doses (0.7 mg-PO_4/L and 1.2 mg-PO_4/L) at two manganese levels (< 6 μg/L and 250 μg/L) on lead release were investigated during this experiment, under both stagnated and flowing water conditions. Key results from this chapter include:

- Influent lead was found to represent only a small fraction of the total lead measured in the effluent waters (1.4 – 6.7%), implying most of the lead measured in the pipe discharge stemmed from lead release.

- The addition of manganese resulted in an increase in lead release, with median bulk water lead concentrations increasing by 13.4% at the 0.7 mg-PO_4/L dose and 83.1% at the 1.2 mg-PO_4/L dose. These results suggest manganese is obstructing

the formation of insoluble Pb(IV) scales and is possibly mobilizing lead into solution.

- PO_4 significantly decreased lead release under the low manganese condition only. An 80.1% reduction in lead release was observed at the low manganese level, with only an 11.9% reduction observed at the high manganese level. The reduced efficacy of PO_4 under the high manganese condition suggests manganese is interacting with phosphate and is reducing its ability to passivate Pb-pipe surfaces.

- Under all experimental conditions, stagnation was shown to significantly increase bulk water lead concentrations by over an order of magnitude. Stagnation also led to significant increases in turbidity, discoloration and the presence of visually detectable lead particles in the bulk water.

- Similar trends observed during the flowing water conditions were observed following the 6-hour stagnation period. The addition of manganese significantly increased bulk water lead concentrations, while decreases observed with the addition of PO_4 were found to be insignificant.

Chapter 7: CONCLUSION

7.1 Synthesis and Conclusions

The purpose of this study was to investigate the fate of manganese in distribution and its potential impact on biomass accumulation and lead release. Experiments were conducted at the bench-scale using annular reactors and lead pipe sections in two independent experimental designs. A study located at the JD Kline Water Supply Plant used untreated source water to confirm biofouling of their raw water transmission pipe. This experimental approach examined the importance of manganese oxidizing bacteria on the accumulation of manganese in distribution, along with the impact of hydraulic changes, cold water conditions and oxidant enhancement on biofilm densities. A second experimental study investigated the impact of orthophosphate and manganese concentrations on manganese and biomass accumulation in distribution. Lead pipe sections were run in series of these reactors to study the impact of residual manganese and phosphate on lead pipes. The key findings from these experimental approaches are summarized in Table 7.1.

Table 7.1 Key findings from each experimental approach.

Chapter	Experimental Approach	Key Findings
Chapter 4: Manganese-biofouling of raw water transmission pipelines	Annular reactors	• Significant manganese accumulation occurred across the transmission pipe, reaching a final density of 115.93 μg/cm^2. • A strong Pearson correlation between MOB and manganese surface densities confirmed biologically facilitated oxidation. • Biofilms were shown to be vulnerable to increases in flow rate and decreases in water temperature. • The rate of manganese accumulation increased by 89% with oxidant enhancement; however, increased water temperatures may have been a contributing factor.
Chapter 5: Impact of phosphate and manganese on biofilm accumulation on polycarbonate surfaces	Annular reactors	• Increasing phosphate doses resulted in a decrease in manganese and manganese oxidizing bacteria accumulation. • Biofilm manganese and MOB densities were strongly correlated, suggesting biologically facilitated oxidation. • Biofilm microbial populations increased with increasing phosphate dose, confirming its role as a nutrient source. • Results suggest phosphate also acted as a sequestering agent, reducing the oxidation of bulk water manganese.

Chapter	Experimental Approach	• Key Findings
Chapter 6: Impact of residual phosphate and manganese on downstream lead pipes	Annular reactors & lead pipe sections	• The addition of manganese resulted in an increase in lead release, with median bulk water concentrations increasing by up to 81%. • Phosphate significantly decreased lead release at the low manganese level. • Stagnation increased bulk water lead by over an order of magnitude and was accompanied by aesthetic deterioration. • The results suggest manganese is competing with phosphate ions, reducing its ability to passivate pipe surfaces.

.

7.2 Recommendations

With the confirmation of manganese-biofouling of the JD Kline Water Supply Plant's raw water transmission pipe, mitigation options now need to be explored. The removal of biofilm caused by the flow rate increase suggests that periodic unidirectional flushing could be the most cost effective option for Halifax Water. Other options warranting further research include determining the water chemistry and hydraulic conditions that promote the greatest biofilm stability and perhaps the inactivation of biofilm through chlorine disinfection. Cold water temperatures were also found to have a negative effect on manganese oxidizing bacteria during this study. Future research could investigate optimization strategies to improve biological manganese oxidation under cold water conditions in the hope of reducing the release of manganese and bacteria into the bulk water phase during inactivation. This research which would also be beneficial to facilities using biofiltration treatment for Mn and organic removal under cold water conditions.

The presence of manganese in drinking water warrants public health concern, as lead release was significantly increased by the addition of manganese within lead pipe sections. Manganese concentrations as low as 6 μg/L were shown to accumulate in appreciable quantities in this study; therefore, water treatment facilities should prioritize manganese removal to reduce the amount of manganese entering distribution. Future research should investigate the relationship between manganese and lead within biofilms, especially in the presence of phosphate based corrosion inhibitors. Optimum phosphate doses should also be explored, as phosphate was shown to interact with both bacteria as a

nutrient source and with manganese as sequestering agent. The competition of phosphate with water constituents other than lead is likely limiting its efficacy as a corrosion inhibitor.

REFERENCES

Adams, L., & Ghiorse, W. (1987). Characterization of extracellular Mn^{2+}-oxidizing activity and isolation of an Mn^{2+}-oxidizing protein from *Leptothrix discophora* SS-1. *Journal of Bacteriology, 169*, 1279-1285.

Bhang, S.-Y., Cho, S.-C., Kim, J.-W., Hong, Y.-C., Shin, M.-S., Yoo, H., Kim, B.-N. (2013). Relationship between blood manganese levels and children's attention, cognition, behavior, and academic performance—A nationwide cross-sectional study. *Environmental Reseach, 126*, 9-16.

Bouchard, M., Sauvé, S., Barbeau, B., Legrand, M., Brodeur, M.-E., Bouffard, T., Mergler, D. (2011). Intellectual impairment in school-age children exposed to manganese from drinking water. *Environmental Health Perspectives, 119*(1), 138-143.

Brandhuber, P., Clark, S., Knocke, W., & Tobiason , J. (2013). *Guidance for the treatment of manganese.* Denver: Water Research Foundation .

Brandhuber, P., Craig, S., Friedman, M., Hill, A., Booth, S., & Hanson, A. (2015). *Legacy of manganese accumulation in water systems.* Denver: Water Research Foundation.

Burger , M., Krentz, C., Mercer, S., & Gagnon , G. (2008). Manganese removal and occurrence of manganese oxidizing bacteria in full-scale biofilters. *Journal of Water Supply: Research and Technology-AQUA, 57*(5), 351.

Camper, A., Brastrup, K., Sandvig, A., Clement, J., Spencer, C., & Capuzzi, A. (2003). Effect of distribution system materials on bacterial regrowth. *Journal AWWA, 95*(7), 107-121.

Carlson, K., Knocke, W., & Gertig, K. (1997). Optimizing treatment through Fe and Mn fractionation. *Journal AWWA, 89*(4), 162-171.

Cartier, C., Nour, S., Richer, B., Deshommes, E., & Prevost, M. (2012). Impact of water treatment on the contribution of faucets to dissolved and particulate lead release at the tap. *Water Research, 46*, 5205-5216.

Caspi, R., Tebo, B., & Haygood, M. (1998). c-type cytochromes and manganese oxidation in *Pseudomonas putida* strain MnB1. *Applied and Environmental Microbiology, 64*, 3549-3555.

Cerrato, J., Falkinham, J., Dietrich, A., Knocke, W., McKinney, C., & Pruden, A. (2010). Manganese-oxidizing and -reducing microorganisms isolated from biofilms in chlorinated drinking water systems. *Water Research, 44*, 3935-3945.

Cerrato, J., Reyes, L., Alvarado, C., & Dietrich, A. (2006). Effect of PVC and iron materials on Mn(II) deposition in drinking water distribution systems. *Water Research, 40*, 2720– 2726.

Chen, Z., Lee, G., & Liu, J. (2000). The effects of chemical remediation treatments on the extractability and speciation of cadmium and lead in contaminated soils. *Chemosphere, 41*, 234-242.

Chu, C., Lu, C., & Lee, C. (2005). Effects of inorganic nutrients on the regrowth of heterotrophic bacteria in drinking water distribution systems. *Journal of Environmental Management, 74*, 255-263.

Dalvi, A., Ajith, N., Swain, K., & Verma, R. (2015). Sorption of arsenic on manganese dioxide synthesized by solid state reaction. *Journal of Environmental Science and Health , Part A, 50*, 866-873.

Dick, G., Torpey, J., Beveridge, T., & Tebo, B. (2008). Direct identification of a bacterial manganese(II) oxidase, the multicopper oxidase MnxG, from spores of several different marine *Bacillus* species. *Applied and Environmental Microbiology, 74*(5), 1527-1534.

Dickinson, W., & Lewandowski, Z. (1996). *Manganese biofouling of stainless steel: deposition rates and influence on corrosion processes.* Houston, Texas: United States: NACE International.

Dong, D., Derry, L., & Lion, L. (2003). Pb scavenging from a freshwater lake by Mn oxides in heterogeneous surface coating materials. *Water Research, 37*, 1662-1666.

Ehrlich, H. (1968). Bacteriology of manganese nodules II. Manganese oxidation by cell-free extract from a manganese nodule bacterium. *Applied Microbiology, 16*(2), 197-202.

Evens, A., Hryhorczuk, D., Lanphear, B., Rankin, K., Lewis, D., Forst, L., & Rosenberg, D. (2015). The impact of low-level lead toxicity on school performance among children in the Chicago Public Schools: a population-based retrospective cohort study. *Enivironmental Health , 14*(1), 1-9.

Fang, W., Hu, J., & Ong, S. (2009). Influence of phosphorus on biofilm formation in model drinking water distribution systems. *Journal of Applied Microbiology, 106*, 1328-1335.

Federal-Provincial-Territorial Committee on Drinking Water . (2016). *Manganese in Drinking Water* . Health Canada .

Feng, X., Zhai, L., Tan, W., Liu, F., & He, J. (2007). Adsorption and redox reactions of heavy metals on synthesized Mn oxide minerals. *Environmental Pollution, 147*, 366-373.

Francis, C., Casciotti, K., & Tebo, M. (2002). Localization of Mn(II)-oxidizing activity and the putative multicopper oxidase, MnxG, to the exosporium of the marine *Bacillus sp*. strain SG-1. *Archives of Microbiology, 178*, 450-456.

Friedman , M., Hill, A., Martel, K., Holt, D., Smith , S., Ta, T., Camper, A. (2003). *Establishing site-specific flushing velocities.* Denver: AWWA Research Foundation.

Friedman, M., Hill, A., Reiber, S., Valentine, R., Larsen, G., Young, A., Peng, C.-Y. (2010). *Assessment of inorganics accumulation in drinking water system scales and sediments.* Denver: Water Research Foundation.

Gagnon, G., Rand, J., O'Leary, K., Rygel, A., Chauret, C., & Andrews, R. (2005). Disinfectant efficacy of chlorite and chlorine dioxide in drinking water biofilms. *Water Research, 39*, 1809-1917.

Garny, K., Horn, H., & Neu, T. (2008). Interaction between biofilm development, structure and detachment in rotating annular reactors. *Biprocess Biosystems Engineering, 31*, 619-629.

Gerke, T., Little, B., & Maynard, J. (2016). Manganese deposition in drinking water distribution systems. *Science of the Total Environment, 541*, 184–193.

Ghiorse, W. (1984). Biology of iron- and manganese- depositing bacteria. *Annual Review of Microbiology, 38*, 515–550.

Ghiorse, W., & Hirsch, P. (1979). An ultrastructural study of iron manganese deposition associated with extracellular polymers of Pedomicrobium-like bacteria. *Archives of Microbiology, 123*, 213-226.

Ginige, M., Wylie, J., & Plumb, J. (2011). Influence of biofilms on iron and manganese deposition in drinking water distribution systems. *Biofouling, 27*(2), 151-163.

Granger, H. (2013). *Manganese removal from surface water using bench scale biofiltration.* (Master's thesis). Halifax: Dalhousie University.

Groschen, G., Arnold, T., Morrow, W., & Warner, K. (2009). *Occurrence and distribution of iron, manganese, and selected trace elements in ground water in the glacial aquifer system of the northern united states.* Reston: USGS.

Halifax Water . (2016). *Typical Analysis of Pockwock/Lake Major Water 2014-2015.* Retrieved from Halifax: http://www.halifax.ca/HalifaxWater/documents/Pockwock-LakeMajor_2014-2015.pdf

Halifax Water. (2010). *Water Supply and Treatment*. Retrieved from Halifax : http://www.halifax.ca/HalifaxWater/WaterQuality/treatment.php

Hastings, D., & Emerson, S. (1986). Oxidation of manganese by spores of a marine *Bacillus*: kinetic and thermodynamic considerations. *Geochimica et Cosmochimica Acta, 50*, 1819-1824.

Health Canada. (2009). *Guidance on Controlling Corrosion in Drinking Water Distribution Systems.* Ottawa: Health Canada.

Health Canada. (2016). *Manganese in Drinking Water.* Federal-Provincial-Territorial Committee on Drinking Water.

Health Canada. (2017). *Guidelines for Canadian Drinking Water Quality—Summary Table.* Water and Air Quality Bureau, Healthy Environments and Consumer Safety Branch, Health Canada, Ottawa, Ontario.

Heintze, S. (1968). Manganese-phosphate reactions in aqueous systems and the effects of application of monocalcium phosphate on the availability of manganese to oats in an alkaline fen soil. *Plant and Soil, 29*(3), 407-423.

Henn, B., Schnaas, L., Ettinger, A., Schwartz, J., Lamadrid-Figueroa, H., Hernández-Avila, M.,Téllez-Rojo, M. (2012). Associations of early childhood manganese and lead coexposure with neurodevelopment. *Environmental Health Perspectives, 120*(1), 126-131.

Hill, A., Friedman, M., Reiber, S., Korshin, G., & Valentine, R. (2010). Behaviour of trace inorganic contaminants in drinking water distribution systems. *Journal AWWA*, 107-118.

Hullo, M., Moszer, I., Danchin, A., & Martin-Verstraete, I. (2001). CotA of *Bacillus subtilis* is a copper-dependent laccase. *Journal of Bacteriology, 183*, 5426-5430.

Jang, H.-J., Choi, Y.-J., Ro, H.-M., & Ka, J.-O. (2012). Effects of phosphate addition on biofilm bacterial communities and water quality in annular reactors equipped with stainless steel and ductile cast iron pipes. *The Journal of Microbiology , 50*(1), 17-28.

Khan, K., Factor-Litvak, P., Wasserman, G., Liu, X., Ahmed, E., Parvez, F., Graziano, J. (2011). Manganese exposure from drinking water and children's classroom behavior in Bangladesh. *Environmental Health Perspectives, 119*(10), 1501-1506.

Kielemoes, J., Bultinck, I., Storms, H., Boon, N., & Verstraete, W. (2002). Occurrence of manganese-oxidizing microorganisms and manganese deposition during biofilm formation on stainless steel in a brackish surface water. *FEMS Microbiology Ecology, 39*, 41-55.

Kim, Y., Kim, B.-N., Hong, Y.-C., Shin, M.-S., Yoo, H.-J., Kim, J.-W., Cho, S.-C. (2009). Co-exposure to environmental lead and manganese affects the intelligence of school-aged children. *NeuroToxicology, 30*, 564-571.

Knocke, W., Hoehn, R., & Sinsabaugh, R. (1987). Using alternative oxidants to remove dissolved manganese for waters laden with organics. *Journal AWWA, 80*(12), 75-79.

Knocke, W., Van Benschoten , J., & Kearney, M. (1990). *Alternative oxidants for the removal of soluble iron and manganese.* Denver : Water Research Foundation and AWWA .

Knowles, A., Nguyen, C., Edwards, M., Stoddart, A., McIlwain, B., & Gagnon, G. (2015). Role of iron and aluminum coagulant metal residuals and lead release from drinking water pipe materials. *Journal of Environmental Science and Health, Part A, 50*, 414-423.

Kogo, A., Payne, S., & Andrews, R. (2017). Comparison of three corrosion inhibitors in simulated partial lead service line replacements. *Journal of Hazardous Materials, 329*, 211-221.

Kohl, P., & Dixon, D. (2012). *Occurrence, impacts and removal of manganese in biofiltration processes.* Denver: Water Research Foundation.

Kohl, P., & Medlar, S. (2006). *Occurrence of manganese in drinking water and manganese control.* Denver: AWWA Research Foundation.

Kwon, K., Refson, K., & Sposito, G. (2013). Understanding the trends in transition metal sorption by vacancy sites in birnessite. *Geochimica et Cosmochimica Acta, 101*, 222-232.

Lauderdale, C., Pope, G., Scheitlin, K., Zwerneman, J., Carollo Engineers, Inc., Kirsits, M., & Bae, S. (2016). *Optimizing filter conditions for improved manganese control during conversion to biofiltration.* Denver: Water Research Foundation.

Lehtola, M., Miettinen, I., & Martikaninen, P. (2002). Biofilm formation in drinking water affected by low concentrations of phosphorous. *Canadian Journal of Microbiology, 48*(6), 494-499.

Lytle, D., & Schock, M. (1996). *Stagnation time, composition, pH and orthophosphate effects on metal leaching from brass.* Cincinnati : USEPA.

Lytle, D., & Schock, M. (2005). The Formation of Pb(IV) Oxides in Chlorinated Water. *2005 AWWA WQTC Conference, Quebec City, QC* (p. 15 p). Denver: AWWARF.

Lytle, D., & Schock, M. (2008). Pitting corrosion of copper in water with high pH and low alkalinity. *Journal AWWA, 100*(3), 115-129.

Lytle, D., & Snoeyink, V. (2002). Effect of ortho- and polyphosphates on the properties of iron particles and suspensions. *Jounrnal AWWA, 94*(10), 87-99.

Manceau, A., Charlet, L., Boisset, M., Didier, B., & Spadini, L. (1992). Sorption and speciation of heavy metals on hydrous Fe and Mn oxides. From microscopic to macroscopic. *Applied Clay Science, 7*, 201-223.

Mandernack, K., Post, J., & Tebo, B. (1995). Manganese mineral formation by bacterial spores of the marine *Bacillus*, strain SG-1: Evidence for the direct oxidation of Mn(II) to Mn(IV). *Geochimica et Cosmochimica Acta, 59*(21), 4393-4408.

McGill, R., Tukey, J., & Larsen, W. (1978). Variations of Box Plots. *The American Statistician , 32*(1), 12-16.

McKenzie, R.M. (1980). The adsorption of lead and other heavy metals on oxides of manganese and iron. *Australian Journal of Soil Research, 18*, 61-73.

McNeill, L., & Edwards, M. (2002). Phosphate inhibitor use at US utilities. *Journal AWWA, 94*(7), 57-63.

McNeill, L., & Edwards, M. (2004). Importance of Pb and Cu particulate species for corrosion control. *Journal of Environmental Engineering, 130*, 136-144.

Miyata, N., Tani, Y., Sakata, M., & Iwahori, K. (2007). Microbial manganese oxide formation and interaction with toxic metal ions. *Journal of Bioscience and Bioengineering, 104*(1), 1-8.

MWH. (2005). *Water treatment principles and design* . Hoboken, NJ, USA: John Wiley and Sons .

NAS. (1973). *Medical and biological effects of environmental pollutants: manganese.* Washington : National Academy of Sciences, National Academy Press.

Nealson, K., & Saffarini, D. (1994). Iron and manganese in anaerobic respiration environmental significance, physiology, and regulation. *Annual Review of Microbiology, 48*, 311-343.

Nealson, K., Tebo, B., & Rosson, R. (1988). Occurrence and mechanisms of microbial oxidation of manganese. *Advances in Applied Microbiology, 33*, 279-318.

Nelson, Y., Lion, L., Ghiorse, W., & Shuler, M. (1999). Production of biogenic Mn oxides by *Leptothrix discophora* SS-1 in a chemically defined growth medium and evaluation of their Pb adsorption characteristics. *Applied and Environmental Microbiology, 65*(1), 175-180.

Nelson, Y., Lion, L., Shuler, M., & Ghiorse, W. (1999). Lead binding to metal oxide and organic phases of natural aquatic biofilms. *Limnology and Oceanography, 44*(7), 1715–1729.

O'Reilly, S., & Hochella, M. J. (2003). Pb sorption efficiencies of natural and synthetic Mn and Fe-oxides. *Geochimica et Cosmochimica Acta, 67*, 4471-4487.

Parikh, S., & Chorover, J. (2005). FTIR spectroscopic study of biogenic Mn-oxide formation by Pseudomonas putida GB-1. *Geomicrobiology Journal, 22*, 207-218.

Parks, J., Kashyap, A., Atassi, A., Schneider, O., & Edwards, M. (2012). Effect of zinc and orthophosphate corrosion inhibitors on cement-based pipes. *Journal AWWA*, E1-E14.

Payne, S. (2013). *Interactions of corrosion control and biofilm on lead and copper in premise plumbing.* (Doctoral thesis). Halifax: Dalhousie University.

Peng, C., Korshin, G., Valentine, R., Hill, A., Friedman, M., & Reiber, S. (2010). Characterization of elemental and structural composition of corrosion scales and deposits formed in drinking water distribution systems. *Water Research*, 4570-4580.

Pieper, K., Tang, M., & Edwards, M. (2017). Flint water crisis caused by interrupted corrosion control: investigating "ground zero" home. *Environmental Science and Technology , 51*, 2007-2014.

Post, J. (1999). Manganese oxide minerals: crystal structures economic and environmental significance. *Proceedings of the National Academy of Sciences of the United States of America, 96*(7), 3447-3454.

Puppa, L., Komarek, M., Bordas, F., Bollinger, J.-C., & Joussein, E. (2013). Adsorption of copper, cadmium, lead and zinc onto a synthetic manganese oxide. *Journal of Colloid and Interface Science, 399*, 99-106.

Rand, J., Hoffman , R., Alam, M., Chauret, C., Cantwell, R., Andrews, R., & Gagnon, G. (2007). A field study evaluation for mitigating biofouling with chlorine dioxide or chlorine integrated with UV disinfection. *Water Research, 41*(9), 1939-1948.

Richardson, L., Aguilar, C., & Nealson, K. (1988). Manganese oxidation in pH and O2 microenvironments produced by phytoplankton. *Limnology Oceanography, 33*(3), 352-363.

Rygel, A. (2006). *Manganese in drinking water distribution* . (Doctoral thesis). Halifax : Dalhousie University.

Sain, A., Griffin, A., & Dietrich, A. (2014). Assessing taste and visual perception of Mn(II) and Mn(IV). *Journal AWWA, 106*(1), E32-E40.

Sawyer, C., McCarty, P., & Parkin, G. (2001). *Chemistry for environmental engineering.* New York: McGraw Hill.

Schock, M. (1989). Understanding corrosion control strategies for lead. *Journal AWWA*, 88-100.

Schock, M. (2005). Distribution systems and reservoirs and reactors for inorganic contaminants. In M. Schock, *Distribution Water Quality Challenges in the 21st Century* (Chapter 6). Denver: AWWA.

Schock, M., Cantor, A., Triantafyllidou, S., Desantis, M., & Scheckel, K. (2014). Importance of pipe deposits to Lead and Copper Rule compliance. *Journal AWWA, 106*(7), E336-E349.

Schock, M., Hyland, R., & Welch, M. (2008). Occurence of contaminant accumulation in lead pipe scales from domestic drinking-water distribution systems. *Environmental Science & Technology, 42*(12), 4285-4291.

Sharp, R., Camper, A., Crippen , J., Schneider , J., & Leggiero, S. (2001). Evaluation of drinking water biostability using biofilm methods. *Journal of Environmental Engineering , 127*(5), 403-411.

Shin, D.-W., Kim, E.-J., Lim, S.-W., Shin, Y.-C., Oh, K.-S., & Kim, E.-J. (2015). Association of hair manganese level with symptoms in attention-deficit/hyperactivity disorder. *Korean Neuropsychiatric Association, 12*(1), 66-72.

Sly, L., Hodgkinson, M., & Arunpairojana, V. (1988). Effect of water velocity on the early development of manganese- depositing biofilm in a drinking-water distribution system. *FEMS Microbiology Ecology, 53*, 175-186.

Sly, L., Hodgkinson, M., & Arunpairojana, V. (1990). Deposition of manganese in a drinking water distribution system. *Applied and Environmental Microbiology, 56*, 628-639.

Stokes, P., Campbell, P., Schroeder, W., Trick, W., France, R., Puckett, K., Donaldson, J. (1988). *Manganese in the Canadian environment* . NRCC (ed.).

Sunda, W., & Kieber, D. (1994). Oxidation of humic substances by manganese oxides yields low-molecular-weight organic substrates. *Naure, 367*, 62-64.

Tebo, B., Bargar, J., Clement, B., Dick, G., Murray, K., Parker, D., Webb, S. (2004). Biogenic manganese oxides: properties and mechanisms of formation. *Annual Review of Earth and Planetary Sciences, 32*, 287-328.

Tebo, B., Johnson, H., McCarthy, J., & Templeton, A. (2005). Geomicrobiology of manganese(II) oxidation. *TRENDS in Microbiology, 13*(9), 421-428.

Tipping, E. (1984). Temperature dependence of Mn(II) oxidation in lakewaters: a test of biological involvement. *Geochimica et Cosmochimica Act, 48*, 1353-1356.

Tobiason, J., Bazilio , A., Goodwill, J., Mai, X., & Nguyen, C. (2016). Manganese Removal from Drinking Water Sources. *Current Pollution Reports, 2*(3), 168-177.

Triantafyllidou, S., Parks, J., & Edwards, M. (2007). Lead Particles in Potable Water. *Journal AWWA, 99*(6), 107-117.

Trueman , B., & Gagnon, G. (2016). Understanding the role of particulate iron and lead release to drinking water . *Environmental Science and Technology, 50*(17), 9053-9060.

Trueman, B., Sweet, G., Harding, M., Estabrook, H., Bishop, D., & Gagnon, G. (2017). Galvanic corrosion of lead by iron (oxyhydr)oxides: potential impacts on drinking water quality. *Environmental Science and Technology, 51*(12), 6812-6820.

USEPA. (2006). *Inorganic contaminant accumulation in potable water distribution systems.* Washington: USEPA.

van Veen, W., Mulder, E., & Deinema, M. (1978). The *Sphaerotilus-Leptothrix* group of bacteria. *Microbiological Review, 42*, 329-356.

van Waasbergen, L., Hildebrand, M., & Tebo, B. (1996). Identification and characterization of a gene cluster involved in manganese oxidation by spores of the marine *Bacillus* sp. strain SG-1. *Journal of Bacteriology, 178*, 3517-3530.

Villalobos, M., Bargar, J., & Sposito, G. (2005). Mechanisms of Pb(II) sorption on a biogenic oxide. *Environmental Science & Technology, 39*, 569-576.

Villalobos, M., Lanson, B., Manceau, A., Toner, B., & Sposito, G. (2006). Structural model for the biogenic Mn oxide produced by *Pseudomonas putida*. *American Mineralogist, 91*, 489-502.

Volk, C., Dundore, E., Schiermann, J., & Lechevallier, M. (2000). Practical evaluation of iron corrosion control in a drinking water distribution system. *Water Research, 34*, 1967-1974.

Wang, Y., Feng, X., Villalobos, M., Tan, W., & Fan, L. (2012). Sorption behavior of heavy metals on birnessite: Relationship with its Mn average oxidation state and implications for types of sorption sites. *Chemical Geology*, 25-34.

Woszczynski, M., Bergese, J., & Gagnon, G. (2013). Comparison of chlorine and chloramines on lead release from copper pipe rigs. *Journal of Environmental Engineering, 139*(8), 1099-1107.

Woszczynski, M., Bergese, J., Payne, S., & Gagnon, G. (2015). Comparison of sodium silicate and phosphate for controlling lead release from copper pipe rigs. *Canadian Journal of Civil Engineering, 42*, 953-959.

Zhang, G., Qu, J., Liu, H., Liu, R., & Wu, R. (2007). Preparation and evaluation of a novel Fe–Mn binary oxide adsorbent for effective arsenite removal. *Water Research, 41*, 1921-1928.

Zhao, D., Yang, X., Zhang, H., Chen, C., & Wang, X. (2010). Effect of environmental conditions on Pb(II) adsorption on B-MnO2. *Chemical Engineering Journal, 164*, 49-55.